

SIZE EFFECT THEORY AND ITS APPLICATION TO FRACTURE OF FIBER COMPOSITES AND SANDWICH PLATES

By Zdeněk P. Bažant¹

Summary. The objective of this article is to summarize a large part of the material presented in an advanced course in Cachan in September 2000. However, not all the material presented in that course is expounded, not only for limitations of scope but other recent sources published by the author are available. The article begins by a broad overview of the problem of size effect or scaling of failure, which has recently come to the forefront of attention in the theory of composites, in view of the efforts to design load bearing composited structures for ships and aircraft. After the overview, attention is focused on the size effect in compression failure of fiber composites occurring in the form of kink bands with fiber microbuckling. The limitations of the Weibull statistical theory of random strength are also spelled out. The presentation is accompanied by selected comparisons with test results and numerical computations.

1 Introduction

The size effect is a problem of scaling. It is a fundamental question in every physical theory. In solid mechanics research, though, little attention has been paid to the deterministic aspects of this problem until recently, although the classical size effect of the randomness of material strength is a classical problem of a very long history. The modern studies of the nonclassical, deterministic size effects, begun in the 1970's, were stimulated by the problems concrete structures, for which there inevitably is a large gap between the scales of large structures (e.g. dams, reactor containments, bridges) and of laboratory tests. This gap involves in such structures about one order of magnitude. In the rare cases of full scale tests, it is impossible to acquire a sufficient statistical basis for generalizing.

In most of mechanical and aerospace engineering, the problem of scaling has been less pressing because the structures or structural components can usually be tested at full size. It must be noted, though, that even in these applications the scaling implied by the theory must be correct. If the scaling properties of a theory are incorrect, the theory is invalid. Recently, the size effect problem acquired prominence in the efforts to design fiber composites and sandwich shells for large ship hulls, bulkheads, decks, stacks and masts, as well as for large load-bearing fuselage panels.

The size effect in solid mechanics is understood as the effect of the characteristic structure size (dimension) D on the nominal strength σ_N of structure when geometrically similar structures are compared. The nominal stress (or strength, in case of maximum load) is defined as $\sigma_N = c_N P/bD$ or $c_N P/D^2$ for two- or three-dimensional similarity, respectively; P = load (or load parameter), b structure thickness, and c_N arbitrary coefficient chosen for convenience (normally $c_N = 1$). So σ_N is not real stress but a load parameter having the dimension of stress. The definition of D can be arbitrary (e.g. the beam depth or half-depth, the beam span, the diagonal dimension, etc.) because it does not matter for comparing geometrically similar structures.

¹Walter P. Murphy Professor of Civil Engineering and Materials Science, Northwestern University, Evanston, Illinois 60208; z-bazant@northwestern.edu.

As is well known, the basic scaling laws in physics are power laws in terms of D . Such scaling implies that no characteristic length or size exists in the theory. The classical Weibull (1939) theory of statistical size effect caused by randomness of material strength has this property. During the 1970's it was discovered that a major deterministic size effect, overwhelming, and in fact suppressing, the statistical size effect, can be caused by the stress redistribution caused by a stable propagation of fracture or damage and the inherent energy release. The law of the deterministic size effect provides a way of bridging two different power laws applicable in two adjacent size ranges, and the structure size at which this bridging transition occurs represents a characteristic size.

The material for which this new kind of size effect was identified first, and for which by far the largest experimental base has been assembled, is concrete. In general, a size effect that bridges the small-scale power law for nonbrittle (plastic, ductile) behavior and the large-scale power law for brittle behavior signals the presence of a certain non-negligible characteristic length of the material. This length, which is the quintessential characteristics of quasi-brittleness, is related to the typical size of material inhomogeneities or the fracture process zone (FPZ).

The quasibrittle materials of interest here are the fiber composite. Other quasibrittle materials include rocks, cement mortars, ice (especially sea ice), consolidated snow, various particulate composites, toughened ceramics, fiber-reinforced concretes, dental cements, bone and cartilage, biological shells, stiff clays, cemented sands, grouted soils, coal, paper, wood, wood particle board, various refractories, filled elastomers, and some special tough metal alloys.

From the material design viewpoint, it is important to note that brittle behavior can be changed to quasibrittle by creating or enhancing material inhomogeneities. Such a behavior is desirable because it endows the structure made from a material incapable of plastic yielding with a significant energy absorption capability. Long ago, civil engineers subconsciously but cleverly engineered concrete structures to achieve and enhance quasibrittle characteristics. Most modern 'high-tech' materials achieve quasibrittle characteristics in much the same way—by means of inclusions, embedded reinforcement, and intentional microcracking, as exemplified by transformation toughening of ceramics, analogous to shrinkage microcracking of concrete. They in fact emulate concrete.

The objective of this article is to summarize a part of the material presented in the advanced course in Cachan in September 2000. Not all the material presented in that course is expounded in this article, not only for limitations of scope but also because it is available in two recent review articles (Bažant and Chen 1997, Bažant 1999), in one detailed paper on scaling for composites (Bažant et al. 1999), in one comprehensive recent monograph (Bažant 2001) and, in a detailed textbook fashion, in the comprehensive book by Bažant and Planas (1998). Considerable duplication with these works became inevitable in view of the requirement to provide for the students an article as a background to the course.

2 History of Size Effect up to Weibull

Speculations about the size effect are found in the notebooks of Leonardo da Vinci (1500's) (Williams 1957) and Galileo's book (1638) which founded the mechanics of materials. A major idea was contributed Mariotte (1686) who, on the basis of his extensive experiments, observed that "a long rope and a short one always support the same weight unless that in a long rope there may happen to be some faulty place in which it will break sooner than in a shorter", and proposed the principle

of "the inequality of matter whose absolute resistance is less in one place than another." In other words, the larger the structure, the greater is the probability of encountering in it an element of a given low strength. This idea is the basis of the statistical theory of size effect.

Little progress was achieved for two and half centuries, until Griffith (1921) showed that the nominal strength of glass fibers was raised from 42,300 psi to 491,000 psi when the diameter decreased from 0.0042 in. to 0.00013 in., and concluded that "the weakness of isotropic solids...is due to the presence of discontinuities or flaws... This conclusion explains Mariotte's statistical idea physically.

The statistical theory of size effect was made possible by the development of extreme value statistics, or the weakest-link model for a chain, in the works of Tippett (1925), Fischer and Tippett (1928), Peirce (1926), and Fréchet (1927), and refined by von Mises (1936) and others (see also Freudenthal 1968, Freudenthal and Gumbell 1956, Selected Papers 1981, Evans 1978). Fischer and Tippett (1928) derived what became later known as the Weibull distribution and showed that this distribution is necessary under a very broad and widely Applicable assumption. The development culminated in the work of Weibull (1939) (also Weibull 1949, 1951, 1956) who, on a heuristic and experimental basis, concluded that the tail distribution of low material strength values with an extremely small probability could not be adequately represented by any of the previously known distributions and independently proposed to characterize it the distribution now called Weibull's. Others (e.g., Freudenthal 1968; Selected Papers 1981) later refined the theoretical justification by analyzing the statistical distribution of microscopic flaws or microcracks. Applications to metals and ceramics, particularly to fatigue embrittlement, cleavage toughness of steels at low and brittle-ductile transition temperatures, evaluation of scatter of fracture toughness data, have been advancing until today; see, e.g. Evans 1978, Beremin 1983, Ruggieri and Dodds 1996, Lei et al. 1998, Kittl and Diaz 1988, 1990. Applications to concrete have also been studied (Zaitsev and Wittmann 1974; Mihashi and Zaitsev 1981, Wittmann and Zaitsev 1981, Zech and Wittmann 1977, Mihashi 1983; Mihashi and Izumi 1977, Carpinteri 1986, 1989, etc.).

Until the mid 1980s, most mechanics paid no attention to the possibility of a deterministic size effect. Whenever a size effect was detected in tests, it was automatically assumed to be statistical, and thus its study was supposed to belong to statisticians rather than mechanics. The subject was not even mentioned by S.P. Timoshenko in 1953 in his monumental History of the Strength of Materials. This negative attitude, however, vanished in the late 1980s.

3 Power Scaling in Absence of Characteristic Length

All the physical systems that involve no characteristic length exhibit a simple power scaling. Consider geometrically similar systems, for example the beams shown in Fig. 1a. We want to deduce the response Y (e.g., the maximum stress or the maximum deflection) as a function of the characteristic size (dimension) D of the structure; $Y = Y_0 f(D)$ where u is the chosen unit of measurement (e.g. 1m, 1mm). We imagine three structure sizes 1, D and D' (Fig. 1a). If we take size 1 as the reference size, the responses for sizes D and D' are $Y = f(D)$ and $Y' = f(D')$. Since there is no characteristic length, we are entitled to alternatively take size D as the reference size. Consequently,

$$f(D')/f(D) = f(D'/D) \quad (1)$$

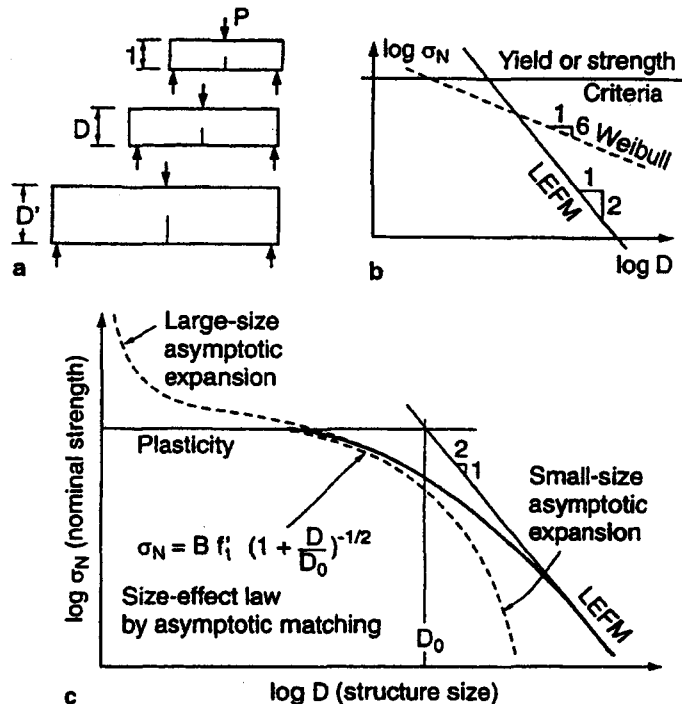


Figure 1: Top left: Geometrically similar structures of different sizes. Top right: Power scaling laws. Bottom: Size effect law for quasibrittle failures bridging the power law of plasticity (horizontal asymptote) and the power law of LEFM (inclined asymptote).

(Bažant 1993, Bažant and Chen 1997 in the context of solids, and Barenblatt 1979, Sedov 1959 in the context of fluid). This is a functional equation which has one and only one solution $f(D)$ —the power law:

$$f(D) = (D/c_1)^s \quad (2)$$

where $s = \text{constant}$ and c_1 is a constant which is always implied as a unit of length measurement (e.g. 1 m, 1 mm).

The power scaling holds true for every physical theory in which there is no characteristic length. In solid mechanics such failure theories include elasticity with a strength limit, elasto-plasticity, viscoplasticity as well as LEFM (for which the FPZ is assumed shrunken into a point).

Note that, on the other hand, function $f(D) = \log(D/c_1)$ does not satisfy equation (1) (and the unit of measurement, c_1 , does not cancel out). Hence, the logarithmic scaling is a possibility only if the system possesses a characteristic length related to c_1 .

To find exponent s , one must take into account the failure criterion of the materia. For elasticity with a strength limit (strength theory), or plasticity (or elasto-plasticity) with a yield surface expressed in terms of stresses or strains, or both, one finds that $s = 0$ when response Y represents the stress or strain (for example the maximum stress, or the stress at certain homologous points, or the nominal stress at failure); Bažant (1993). Thus, if there is no characteristic dimension, all geometrically similar structures of different sizes must fail at the same nominal stress. By convention, this came to be known as the case of *no size effect*. In LEFM, by contrast, $s = -1/2$, provided that the crack or notches are not negligible compared to D and that the geometric similarity applies not only to the external structure shape but also to the cracks or notches (Bažant, 1993).

If $\log \sigma_N$ is plotted versus $\log D$, the power law is a straight line (Fig. 1b). For plasticity, or

elasticity with a strength limit, the exponent of the power law vanishes, i.e., the slope of this line is 0. For LEFM, the slope is $-1/2$. For quasibrittle materials and structures the size effect bridges these two power laws, and bridging range of t principal ingterest .

4 Weibull Statistical Size Effect

The three-dimensional continuous generalization of the weakest link model for the failure of a chain of links of random strength (Fig. 2 left) leads to the distribution (e.g., Bažant 2001, Bažant and Planas 1998):

$$P_f(\sigma_N) = 1 - \exp \left[- \int_V c(\sigma(\mathbf{x}), \sigma_N) dV(\mathbf{x}) \right] \quad (3)$$

which represents the probability that a structure that fails as soon as macroscopic fracture initiates from a microcrack (or a some flaw) somewhere in the structure; σ = stress tensor field just before failure, \mathbf{x} = coordinate vector, V = volume of structure, and $c(\sigma)$ = function giving the spatial concentration of failure probability of the material ($= V_r^{-1} \times$ failure probability of material representative volume V_r) (Freudenthal 1968); $c(\sigma) \approx \sum_i P_1(\sigma_i)/V_0$ where σ_i = principal stresses ($i = 1,2,3$) and $P_1(\sigma)$ = failure probability (cumulative) of the smallest possible test specimen of volume V_0 (or representative volume of the material) subjected to uniaxial tensile stress σ ;

$$P_1(\sigma) = \left\langle \frac{\sigma - \sigma_u}{s_0} \right\rangle^m \quad (4)$$

(Weibull 1939) where m, s_0, σ_u = material constants (m = Weibull modulus, usually between 5 and 50; s_0 = scale parameter; σ_u = strength threshold, which may usually be taken as 0) and V_0 = reference volume understood as the volume of specimens on which $c(\sigma)$ was measured. For specimens under uniform uniaxial stress (and $\sigma_u = 0$), (3) and (4) lead to the following simple expressions for the mean and coefficient of variation of the nominal strength:

$$\bar{\sigma}_N = s_0 \Gamma(1 + m^{-1})(V_0/V)^{1/m}, \quad \omega = [\Gamma(1 + 2m^{-1}) / \Gamma^2(1 + m^{-1}) - 1]^{1/2} \quad (5)$$

where Γ is the gamma function. Since ω depends only on m , it is often used for determining m from the observed statistical scatter of strength of identical test specimens. The expression for $\bar{\sigma}_N$ includes the effect of volume V which depends on size D . In general, for structures with nonuniform multidimensional stress, the size effect of Weibull theory (for $\sigma_r \approx 0$) is of the type:

$$\bar{\sigma}_N \propto D^{-n_d/m} \quad (6)$$

where $n_d = 1, 2$ or 3 for uni-, two- or three-dimensional similarity.

In view of (5), the value $\sigma_W = \sigma_N(V/V_0)^{1/m}$ for a uniformly stressed specimen can be adopted as a size-independent stress measure called the Weibull stress. Taking this viewpoint, Beremin (1983) proposed taking into account the nonuniform stress in a large crack-tip plastic zone by the so-called Weibull stress:

$$\sigma_W = \left(\sum_i \sigma_i^m \frac{V_i}{V_0} \right)^{1/m} \quad (7)$$

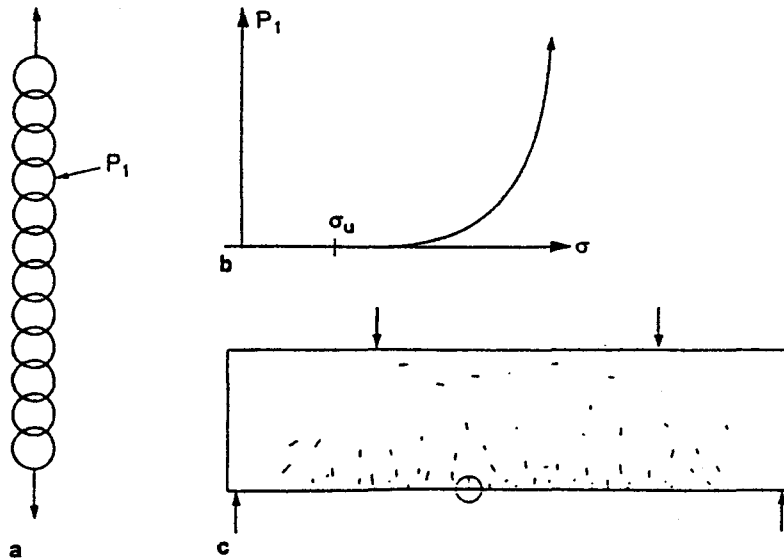


Figure 2: Left: Chain with many links of random strength. Right top: Failure probability of a small element. Right bottom: Structure with many microcracks of different probabilities to become critical.

where V_i ($i = 1, 2, \dots, N_W$) are elements of the plastic zone having maximum principal stress σ_{1i} . Ruggieri and Dodds (1996) replaced the sum in (5) by an integral; see also Lei et al. (1998). Eq. (7), however, considers only the crack-tip plastic zone whose size which is almost independent of D . Consequently, Eq. (7) is applicable only if the crack at the moment of failure is not yet macroscopic, still being negligible compared to structural dimensions.

In the case of quasibrittle structures, applications of the classical Weibull theory face serious objections:

1. The fact that in (6) the size effect is a power law implies the absence of any characteristic length. But this cannot be true if the material contains sizable inhomogeneities.
2. The energy release due to stress redistributions caused by macroscopic FPZ or stable crack growth before P_{max} gives rise to a deterministic size effect which is ignored. Thus the Weibull theory is valid only if the structure fails as soon as a microscopic crack becomes macroscopic.
3. Every structure is mathematically equivalent to a uniaxially stressed bar (or chain, Fig. 2), which means that no information on the structural geometry and failure mechanism is taken into account.
4. The size effect differences between two- and three-dimensional similarity ($n_d = 2$ or 3) are predicted much too large.
5. Many tests of quasibrittle materials (e.g., diagonal shear failure of reinforced concrete beams) show a much stronger size effect than predicted by Weibull theory ([BP], and the review in Bažant 1997a).
6. The classical theory neglects the spatial correlations of material failure probabilities of neighboring elements caused by nonlocal properties of damage evolution (while generalizations based on some phenomenological load-sharing hypotheses have been divorced from mechanics).

7. When (5) is fit to the test data on statistical scatter for specimens of one size ($V = \text{const.}$), and when (6) is fit to the mean test data on the effect of size or V (of unnotched plain concrete specimens), the optimum values of Weibull exponent m are very different, namely $m = 12$ and $m = 24$, respectively (Bažant and Novák, in preparation). If the theory were applicable, these value would have to coincide.

These limitations mean that, among concrete structures, Weibull theory is valid only for extremely thick plain (unreinforced) structures (e.g., arch dams, retaining walls, foundation plinths). These limitations raise questions about many applications of the Weibull theory proposed in the past.

5 Deterministic Size Effect Bridging Plasticity and LEFM

Quasibrittle materials follow on a small scale the theory of plasticity (or strength theory), characterized by material strength or yield limit σ_0 , and on a large scale the LEFM, characterized by fracture energy G_f or fracture toughness K_c . Plasticity alone, as well as LEFM alone, possesses no characteristics length, but the combination of both does. The values of σ_0 and G_f together imply Irwin's (1958) characteristic length (material length):

$$\ell_0 = \frac{EG_f}{\sigma_0^2} = \frac{K_c^2}{\sigma_0^2} \quad (8)$$

which approximately characterizes the size of the FPZ ($E = \text{Young's elastic modulus}$). In dynamics, this further implies the existence of a characteristic time (material time):

$$\tau_0 = \ell_0/v \quad (9)$$

representing the time that a wave of velocity v needs to propagate the distance ℓ_0 .

After LEFM was first applied to concrete (Kaplan 1961), it was found to disagree with test results (Kesler et al. 1971; Leicester 1969; Walsh 1972, 1976). Leicester (1969) tested geometrically similar notched beams of different sizes, fit the results by a power law, $\sigma_N \propto D^{-n}$, and observed that the optimum n was less than 1/2, the value required by LEFM. The power law with a reduced exponent of course fits the test data in the central part of the transitional size range well but does not provide the bridging of the ductile and LEFM size effects. It was tried to explain the reduced exponent value by notches of a finite angle, which however is objectionable for two reasons: (i) notches of a finite angle cannot propagate (rather, a crack must emanate from the notch tip), (ii) the singular stress field of finite-angle notches gives a zero flux of energy into the notch tip. Same as Weibull theory, Leicester's power law also implied nonexistence of a characteristic length (see Bažant and Chen, 1997, Eqs. 1-3), which cannot be the case for concrete due to the large size of its inhomogeneities. More extensive tests of notched geometrically similar concrete beams of different sizes were carried out by Walsh (1972, 1976). Although he did not attempt a mathematical formulation, he was first to trace the experimental curve of nominal strength versus size in a bi-logarithmic plot and observe that it was transitional between the power laws of plasticity and LEFM.

A major advance was made by Hillerborg et al. (1976) (also Petersson 1981). Inspired by the softening and plastic FPZ models of Barenblatt (1959, 1962) and Dugdale (1960), they formulated the cohesive (or fictitious) crack model characterized by a softening stress-displacement law for the

crack opening and showed by finite element calculations that the failures of unnotched plain concrete beams in bending exhibit a deterministic size effect, in agreement with the test data on the modulus of rupture. At the same time, analysis of distributed (smeared) cracking damage (Bažant 1976) demonstrated that its localization into a crack band engenders a deterministic size effect on the postpeak deflections and energy dissipation of structures. The effect of the crack band is approximately equivalent to that of a long fracture with a sizable FPZ at the tip. Subsequently, based on an approximate energy release analysis, the size effect law for the quasibrittle size effect in structures failing after large stable crack growth was derived (Bažant 1984):

$$\sigma_N = B\sigma_0 \left(1 + \frac{D}{D_0}\right)^{-1/2} + \sigma_R \quad (10)$$

$$\text{or more generally: } \sigma_N = B\sigma_0 \left[1 + \left(\frac{D}{D_0}\right)^r\right]^{-1/2r} + \sigma_R \quad (11)$$

in which r , B = positive dimensionless constants; D_0 = constant representing the transitional size (at which the power laws of plasticity and LEFM intersect); D_0 and B characterize the structure geometry. Usually constant $\sigma_R = 0$, except when there is a residual crack-bridging stress σ_r outside the FPZ (as in fiber composites). Eq. (10) was shown to be closely followed by the numerical results for the crack band model (Bažant 1976, Bažant and Oh 1983), as well as those for the nonlocal continuum damage models.

Beginning in the mid 1980s, the interest in the quasibrittle size effect of concrete structures surged enormously and many researchers made noteworthy contributions; to name but a few: Planas and Elices (1988, 1989, 1993), Petersson (1981), and Carpinteri (1986). The size effect has recently become a major theme at conferences on concrete fracture (Bažant, ed., 1992; Mihashi et al., eds., 1994; Wittmann, ed., 1995, Mihashi and Rokugo, eds., 1998) and fiber composites (e.g., Bažant and Rajapakse, 1999).

Matching the measurements of the size effect by the size effect law was shown to offer a simple way to determine the fracture characteristics of quasibrittle materials, including the fracture energy, the effective FPZ length, and the (geometry dependent) R-curve (this method was adopted for an international standard recommendation, RILEM 1990).

6 Dimensional Analysis of Power-Law Size Effect

The exponents of the asymptotic power laws of the transitional size effect can be easily deduced from dimensional analysis. The number of dimensionless variables governing a physical phenomenon can be determined from Buckingham's Π theorem (see Barenblatt 1979, 1987). This theorem states that the number of governing dimensionless variables is equal to the total number of variables minus the number of parameters with independent physical dimensions (in these cases just two, length and force). It readily follows that the condition of failure when only the material strength or yield limit σ_0 governs, with no role for the energy release rate, must have the form:

$$f\left(\frac{\sigma_N}{\sigma_0}, \frac{L_1}{D}, \frac{L_2}{D}, \dots\right) = 0 \quad (12)$$

where f is a certain function and L_1, L_2, \dots are spatial dimensions whose ratios to D characterize the structure geometry. Since σ_0 is a constant and, for geometrically similar structures $L_1/D, L_2/D, \dots$ are constants, too, it follows that the nominal stress at failure, σ_N , must be proportional to σ_0 , and therefore a constant when the structure size D is varied. Note that the material parameters present in the failure condition, which consist of σ_0 alone, imply no characteristic length.

In linear elastic fracture mechanics (LEFM), the failure is determined by the critical stress intensity factor K_c (fracture toughness), the metric dimension of which is $\text{N m}^{-3/2}$. It is straightforward to figure out that the dimensionless failure condition must now have the form

$$\Phi\left(\frac{\sigma_N\sqrt{D}}{K_c}, \frac{L_1}{D}, \frac{L_2}{D}, \dots\right) = 0 \quad (13)$$

where $L_1 = a =$ notch length. Since K_c is a material constant and the ratios $L_1/D, L_2/D, \dots$ are constant as well, for geometrically similar structures, it follows that $\sigma_N\sqrt{D}$ must also be constant. Hence, $\sigma_N \propto D^{-1/2}$ (e.g., Bažant, 1983, 1984; Carpinteri 1984, 1986). Note again that the material parameters present in the failure condition, which consist of K_c alone, imply no characteristic length (together with material strength σ_0 , of course, K_c does imply a material length, $l_{ch} = K_c^2/\sigma_0^2$, but σ_0 is not a parameter in LEFM; it is a parameter in ductile-brittle or quasibrittle fracture mechanics).

The dimensional analysis, unfortunately, becomes ambiguous in some more complex problems, for example the bending failure of floating ice plates, to be discussed later.

For systems with no characteristic dimension, the size effect can also be deduced, without recourse to physics, simply by converting the mathematical formulation of the boundary value problem to a dimensionless form. To this end we introduce the dimensionless variables, labeled by an overbar;

$$\bar{x}_i = x_i/D, \quad \bar{u}_i = u_i/D, \quad \bar{\sigma}_{ij} = \sigma_{ij}/\sigma_0 \quad (14)$$

$$\bar{p}_i = p_i/\sigma_N, \quad \bar{f}_i = f_i D/\sigma_N, \quad \bar{E}_{ijkl} = E_{ijkl}/\sigma_0 \quad (15)$$

where $x_i =$ Cartesian coordinates ($i = 1, 2, 3$), $\sigma_{ij} =$ stress tensor components, $p_i =$ given surface tractions, $f_i =$ body forces, and $E_{ijkl} =$ elastic moduli. The strain components are $\epsilon_{ij} = \frac{1}{2}(u_{i,j} + u_{j,i})$, the field equilibrium equations are $\sigma_{ij,i} + f_j = 0$, and the stress boundary conditions are $n_i\sigma_{ij} = p_i$ on Γ_s , where n_i is the unit surface normal, Γ_s is the surface domain where stresses are prescribed, and the derivatives with respect to x_i are denoted by subscript i preceded by a comma. Denoting the derivatives with respect to dimensionless coordinates as $\partial_i = \partial/\partial\bar{x}_i$, and noting that $\partial/\partial x_i = (1/D)\partial_i$, we can transform the foregoing equations to the following dimensionless form:

$$\bar{\epsilon}_{ij} = \frac{1}{2}(\partial_j\bar{u}_i + \partial_i\bar{u}_j), \quad \partial_j\bar{\sigma}_{ij} + \bar{f}_i = 0 \quad (\text{in } \mathcal{V}) \quad (16)$$

$$n_j\bar{\sigma}_{ij} = \bar{p}_i \quad (\text{on } \Gamma_s), \quad \bar{u}_i = 0 \quad (\text{on } \Gamma_d) \quad (17)$$

where $\bar{\epsilon}_{ij} = \epsilon_{ij}$; \mathcal{V} is the domain of structure volume and Γ_d is the surface domain where the displacements are prescribed as zero. These equations must be complemented by the constitutive law and the material failure condition.

In plasticity, or elasticity with a strength limit, the constitutive law and material failure conditions are expressed as equations and inequalities involving functions of the type $F(\sigma, \epsilon)$ or, in dimensionless form,

$$F(\sigma_N, \bar{\sigma}_{ij}, \bar{\epsilon}_{ij}) \quad (18)$$

where f is a certain function and L_1, L_2, \dots are spatial dimensions whose ratios to D characterize the structure geometry. Since σ_0 is a constant and, for geometrically similar structures $L_1/D, L_2/D, \dots$ are constants, too, it follows that the nominal stress at failure, σ_N , must be proportional to σ_0 , and therefore a constant when the structure size D is varied. Note that the material parameters present in the failure condition, which consist of σ_0 alone, imply no characteristic length.

In linear elastic fracture mechanics (LEFM), the failure is determined by the critical stress intensity factor K_c (fracture toughness), the metric dimension of which is $\text{N m}^{-3/2}$. It is straightforward to figure out that the dimensionless failure condition must now have the form

$$\Phi \left(\frac{\sigma_N \sqrt{D}}{K_c}, \frac{L_1}{D}, \frac{L_2}{D}, \dots \right) = 0 \quad (13)$$

where $L_1 = a =$ notch length. Since K_c is a material constant and the ratios $L_1/D, L_2/D, \dots$ are constant as well, for geometrically similar structures, it follows that $\sigma_N \sqrt{D}$ must also be constant. Hence, $\sigma_N \propto D^{-1/2}$ (e.g., Bažant, 1983, 1984; Carpinteri 1984, 1986). Note again that the material parameters present in the failure condition, which consist of K_c alone, imply no characteristic length (together with material strength σ_0 , of course, K_c does imply a material length, $l_{ch} = K_c^2/\sigma_0^2$, but σ_0 is not a parameter in LEFM; it is a parameter in ductile-brittle or quasibrittle fracture mechanics).

The dimensional analysis, unfortunately, becomes ambiguous in some more complex problems, for example the bending failure of floating ice plates, to be discussed later.

For systems with no characteristic dimension, the size effect can also be deduced, without recourse to physics, simply by converting the mathematical formulation of the boundary value problem to a dimensionless form. To this end we introduce the dimensionless variables, labeled by an overbar;

$$\bar{x}_i = x_i/D, \quad \bar{u}_i = u_i/D, \quad \bar{\sigma}_{ij} = \sigma_{ij}/\sigma_0 \quad (14)$$

$$\bar{p}_i = p_i/\sigma_N, \quad \bar{f}_i = f_i D/\sigma_N, \quad \bar{E}_{ijkl} = E_{ijkl}/\sigma_0 \quad (15)$$

where $x_i =$ Cartesian coordinates ($i = 1, 2, 3$), $\sigma_{ij} =$ stress tensor components, $p_i =$ given surface tractions, $f_i =$ body forces, and $E_{ijkl} =$ elastic moduli. The strain components are $\epsilon_{ij} = \frac{1}{2}(u_{i,j} + u_{j,i})$, the field equilibrium equations are $\sigma_{ij,i} + f_j = 0$, and the stress boundary conditions are $n_i \sigma_{ij} = p_i$ on Γ_s , where n_i is the unit surface normal, Γ_s is the surface domain where stresses are prescribed, and the derivatives with respect to x_i are denoted by subscript i preceded by a comma. Denoting the derivatives with respect to dimensionless coordinates as $\partial_i = \partial/\partial \bar{x}_i$ and noting that $\partial/\partial x_i = (1/D)\partial_i$, we can transform the foregoing equations to the following dimensionless form:

$$\bar{\epsilon}_{ij} = \frac{1}{2}(\partial_j \bar{u}_i + \partial_i \bar{u}_j), \quad \partial_j \bar{\sigma}_{ij} + \bar{f}_i = 0 \quad (\text{in } \mathcal{V}) \quad (16)$$

$$n_j \bar{\sigma}_{ij} = \bar{p}_i \quad (\text{on } \Gamma_s), \quad \bar{u}_i = 0 \quad (\text{on } \Gamma_d) \quad (17)$$

where $\bar{\epsilon}_{ij} = \epsilon_{ij}$; \mathcal{V} is the domain of structure volume and Γ_d is the surface domain where the displacements are prescribed as zero. These equations must be complemented by the constitutive law and the material failure condition.

In plasticity, or elasticity with a strength limit, the constitutive law and material failure conditions are expressed as equations and inequalities involving functions of the type $F(\sigma, \epsilon)$ or, in dimensionless form,

$$F(\sigma_N, \bar{\sigma}_{ij}, \bar{\epsilon}_{ij}) \quad (18)$$

Because D does not appear in (16) and (17), $\bar{\sigma}_{ij}$, $\bar{\epsilon}_{ij}$ are size independent, and because at least some of the functions F are not homogeneous functions, the conditions in terms of these functions can remain valid for all D only if σ_N is a constant. This demonstrates that there is no size effect in plasticity or strength based theories (or any theory in which the material failure condition is expressed solely in terms of stress and strain).

In LEFM, the constitutive law and the failure condition at crack (or notch) tip may be written as $\sigma_{ij} = E_{ijkl}\epsilon_{ij}$ and $\lim(\sigma_{22}\sqrt{2\pi x_1}) = K_c$ for $x_1 \rightarrow 0$; here we assume that the origin of coordinates x_i is placed into the crack tip, x_1 is the direction of propagation and x_2 is normal to the crack plane. Transformation to dimensionless coordinates yields:

$$\sigma_N \bar{\sigma}_{ij} = \sigma_0 \bar{E}_{ijkl} \bar{\epsilon}_{ij}, \quad \sigma_N \sqrt{D} \lim_{x_1 \rightarrow 0} (\bar{\sigma}_{22} \sqrt{2\pi \bar{x}_1}) = K_c \quad (19)$$

The second of these two equations is valid for all sizes D if and only if $\sigma_N \propto 1/\sqrt{D}$, and then the first equation is valid for all D if and only if $\epsilon_{ij} = \bar{\epsilon}_{ij} \propto \sigma_N$ or $\epsilon_{ij} \propto 1/\sqrt{D}$. This establishes the scaling law of LEFM. Instead of the second equation in (19), one could use the condition on critical energy release rate (Bažant 1983), with the same result.

7 Stress Redistribution and Energy Release as a Mechanism of Size Effect

The gist of the deterministic quasibrittle size effect may be explained as follows. LEFM applies when the FPZ is negligibly small compared to structural dimension D and can be considered as a point. Thus the LEFM solutions can be obtained by methods of elasticity. The salient property of quasibrittle materials is that there exists a sizable FPZ with distributed cracking or other softening damage that is not negligibly small compared to structural dimension D . This makes the problem nonlinear.

The existence of a large FPZ means that the distance between the tip of the actual (traction-free) crack and the tip of the equivalent LEFM crack at P_{max} is equal to a certain characteristic length c_f (roughly one half of the FPZ size) that is not negligible compared to D . This causes a non-negligible macroscopic stress redistribution with energy release from the structure.

With respect to the fracture length a_0 (distance from the mouth of notch or crack to the beginning of the FPZ), two basic cases may now be distinguished: (i) $a_0 = 0$, which means that P_{max} occurs at the initiation of macroscopic fracture propagation, and (ii) a_0 is finite and not negligible compared to D , which means that P_{max} occurs after large stable fracture growth.

7.1 Scaling for failure at crack initiation:

The first case is exemplified by the modulus of rupture test, which consists of the flexural failure of a simply supported beam (of span L) with a rectangular cross section (of depth D and width b), subjected to concentrated load P . The maximum load is not decided by the stress $\sigma_1 = 3PL/2bD^2$ at the tensile face, but by the stress value $\bar{\sigma}$ roughly at distance $c_f/2$ from the tensile face (which is at the middle of FPZ). Because $\bar{\sigma} = \sigma_1 - \sigma'_1 c_f/2$ where $\sigma'_1 =$ stress gradient $= 2\sigma_1/D$, and also because $\bar{\sigma} = \sigma_0 =$ intrinsic tensile strength of the material, the failure condition $\bar{\sigma} = \sigma_0$ yields $P/bD = \sigma_N = \sigma_0/(1 - D_b/D)$ where $D_b = (3L/2D)c_f$, which is a constant because for geometrically similar beams

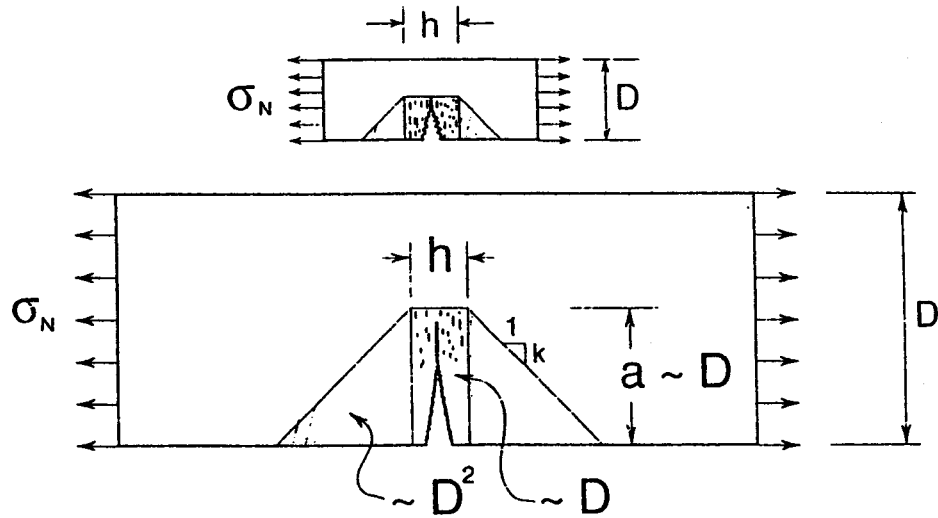


Figure 3: Approximate zones of stress relief due to fracture.

$L/D = \text{constant}$. This expression, however, is unacceptable for $D \leq D_b$. But since the derivation is valid only for small enough c_f/D , one may replace it by the following asymptotically equivalent size effect formula:

$$\sigma_N = \sigma_0 \left(1 + \frac{r D_b}{D} \right)^{1/r} \quad (20)$$

which happens to be acceptable for the entire size range (r is any positive constant). The values $r = 1$ or 2 have been used for concrete (Bažant 1998), while $r \approx 1.45$ is found to be optimum according to Bažant and Novák (2000).

7.2 Scaling for failures with a long crack or notch:

Let us now explain the essence of the size effect for the second case of structures with notches or large traction-free cracks. Failures of this type, exhibiting a strong size effect ([BP], Bažant 1996, Walraven 1995, Iguro et al. 1985, Shioya and Akiyama 1995, Bažant and Kazemi 1991, Gettu et al. 1990, Marti 1989) are typical of reinforced concrete structures, as well as fiber composites (Bažant, Li and Daniel 1986, Wisnom 1992). Consider the rectangular panel in Fig. 3, which is initially under a uniform stress equal to σ_N . Introduction of a crack of length a with a FPZ of a certain length and width h may be approximately imagined to relieve the stress, and thus release the strain energy, from the shaded triangles on the flanks of the crack band shown in Fig. 3. The slope k of the effective boundary of the stress relief zone need not be determined; what is important is that k is independent of the size D .

For the usual ranges of interest, the length of the crack at maximum load may normally be assumed approximately proportional to the structure size D while the size h of the FPZ is essentially a constant, related to the inhomogeneity size in the material. This has been verified for many cases by experiments (showing similar failure modes for small and large specimens) and finite element solutions based on crack band, cohesive or nonlocal models.

The stress reduction in the triangular zones of areas $ka^2/2$ (Fig. 3) causes (for the case $b = 1$)

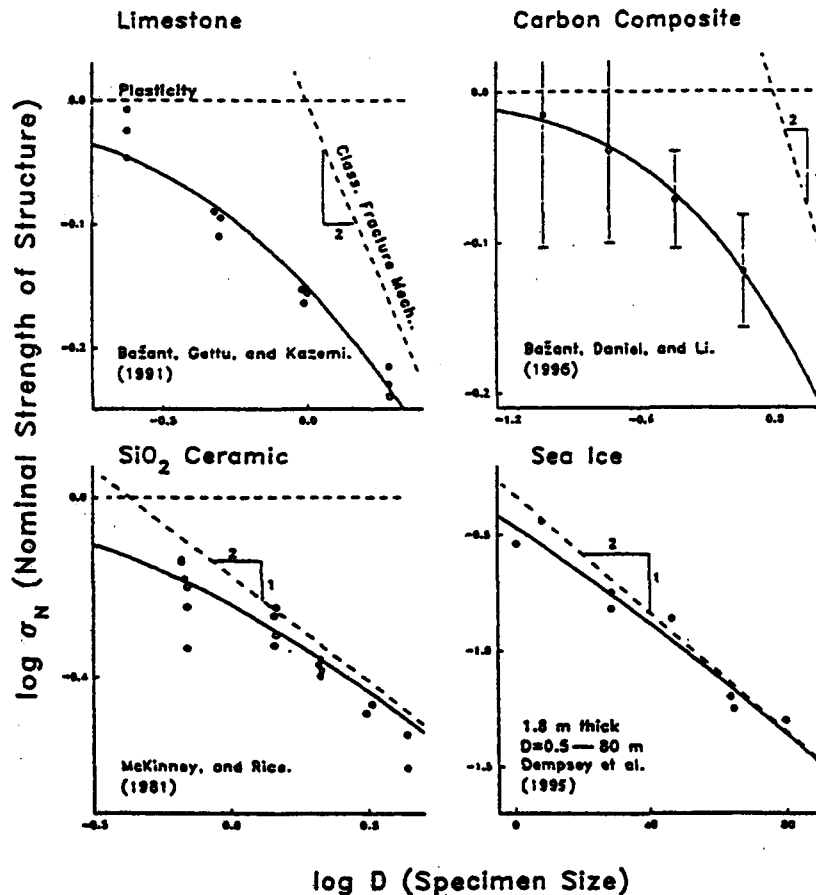


Figure 4: Nominal strength data from the tests of Indiana limestone (Bažant, Gettu and Kazemi 1991), carbon fiber epoxy laminates (Bažant, Daniel and Li 1996), SiO₂ ceramics (McKinney and Rice 1981), and sea ice (Dempsey et al. 1996, 1999, Mulmule et al. 1996), and their fits by the size effect law.

the energy release $U_a = 2 \times (ka^2/2)\sigma_N^2/2E$. The stress drop within the crack band of width h causes further energy release $U_b = hao^2_N/E$. The total energy dissipated by the fracture is $W = aG_f$, where G_f is the fracture energy, a material property representing the energy dissipated per unit area of the fracture surface. Energy balance during static failure requires that $\partial(U_a + U_b)/\partial a = dW/da$. Setting $a = D(a/D)$ where a/D is approximately a constant if the failures for different structure sizes are geometrically similar, the solution of the last equation for σ_N yields Bažant's (1984) approximate size effect law in (10) with $\sigma_R = 0$ (Fig. 1 bottom).

More rigorous derivations of this law, applicable to arbitrary structure geometry, have been given in terms of asymptotic analysis based equivalent LEFM (Bažant 1997b) or on Rice's path-independent J-integral (Bažant and Planas 1998). This law has also been verified by nonlocal finite element analysis, and by random particle (or discrete element) models. The experimental verifications, among which the earliest was provided by the pioneering tests of Walsh (1972, 1976), have by now become abundant (e.g. Fig. 7.2).

For very large sizes ($D \gg D_0$), the size effect law in (10) reduces to the power law $\sigma_N \propto D^{-1/2}$, which represents the size effect of LEFM (for geometrically similar large cracks) and corresponds to the inclined asymptote of slope $-1/2$ in Fig. 1 (bottom). For very small sizes ($D \ll D_0$), this law reduces to $\sigma_N = \text{const.}$, which corresponds to the horizontal asymptote and means that there is no size effect, as in plastic limit analysis.

The ratio $\beta = D/D_0$ is called the brittleness number of a structure. For $\beta \rightarrow \infty$ the structure is perfectly brittle (i.e. follows LEFM), in which case the size effect is the strongest possible, while for $\beta \rightarrow 0$ the structure is non-brittle (or ductile, plastic), in which case there is no size effect. Quasibrittle structures are those for which $0.1 \leq \beta \leq 10$, in which case the size effect represents a smooth transition (or interpolation) that bridges the power law size effects for the two asymptotic cases. The law (10) has the character of asymptotic matching and serves to provide the bridging of scales. In the quasibrittle range, the stress analysis is of course nonlinear, calling for the cohesive crack model or the crack band model (which are mutually almost equivalent), or some of the nonlocal damage models.

The meaning of the term quasibrittle is relative. If the size of a quasibrittle structure becomes sufficiently large compared to material inhomogeneities, the structure becomes perfectly brittle (for concrete structures, only the global fracture of a large dam is describable by LEFM), and if the size becomes sufficiently small, the structure becomes non-brittle (plastic, ductile) because the FPZ extends over the whole cross section of the structure (thus a micromachine or a miniature electronic device made of silicone or fine-grained ceramic may be quasibrittle or non-brittle).

Comparisons of the size effect law (20) with size effect tests of geometrically similar notched specimens of different sizes are shown in Fig. 7.2. This includes a comparison with tests of orthotropic laminates. Further comparisons with tests of laminates at Northwestern University and at the laboratory of Wisnom () can be found in Bažant, Daniel and Li (1996).

8 Use of J-Integral for Asymptotic Scaling Analysis

Rice's J-integral allows the most fundamental derivation of the scaling law and lends itself naturally to a generalization for compressive fracture in which normal stresses are transmitted across the cracking band. However, there is a disadvantage: Unlike the LEFM energy release function $g\alpha$, the J-integral does not capture the shape (geometry) effect and thus does not provide a method to obtain analytical expressions for the coefficients in the size effect law.

Consider geometrically similar structures scaled in two dimensions (the treatment for three dimensions, however, would be analogous). We introduce dimensionless cartesian coordinates (Fig. 8) $\xi_i = x_i/D$ and dimensionless displacements $\zeta_i = u_i$ where $i = 1, 2$. For two-dimensional similarity, the elastic material compliances scale as $C_{ijkl} = c_{ijkl}/E$ where c_{ijkl} are constant.

If c_f were zero, the stresses would scale as $\sigma_{ij} = \sigma_N S_{ij}(\xi)$ where $\xi =$ coordinate vector of ξ_i , and S_{ij} are size-independent functions. However, the presence of nonzero material length c_f will influence the stress distributions. Based on the principles of dimensional analysis, this influence and the influence on the displacement field must have the form:

$$\sigma_{ij} = \sigma_N S_{ij}(\xi, \theta), \quad u_i = (\sigma_N/E) D \zeta_i(\xi, \theta) \quad (21)$$

where $\theta = c_f/D$ and ζ_i are dimensionless functions. The flux of energy into a fracture process zone

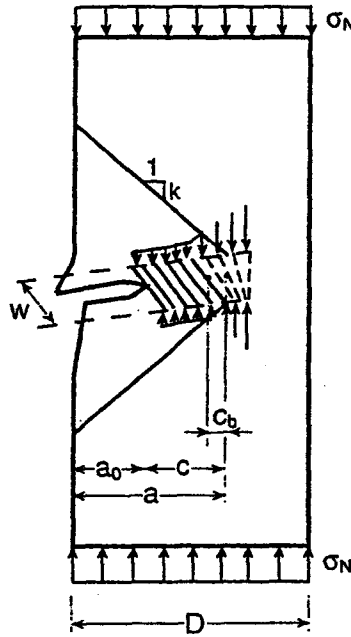


Figure 5: Idealized kink band of width w in a notched specimen, with a fracture process zone of effective length c_b and idealized energy release zone.

advancing in the direction of x_1 (Fig. 8) can be calculated by Rice's J-integral:

$$J = \int_{\Gamma} (W n_1 - n_j \sigma_{ij} u_{i,1}) ds \quad (22)$$

$$= \int_{\Gamma} \left(\frac{1}{2} C_{ijkl} \sigma_{ij} \sigma_{kl} n_1 - n_j \sigma_{ij} \frac{\partial u_i}{\partial x_1} \right) ds \quad (23)$$

$$= \int_{\Gamma} \left(\frac{\sigma_N^2}{2E} c_{ijkl} S_{ij} S_{kl} n_1 - n_j \sigma_N S_{ij} \frac{\sigma_N D}{E} \frac{\partial \zeta_i}{\partial \xi_1} \right) D d\bar{s} \quad (24)$$

$$= \frac{\sigma_N^2 D}{E} \mathcal{J}(\theta), \quad (25)$$

$$\mathcal{J}(\theta) = \int_{\bar{\Gamma}} \left(\frac{1}{2} c_{ijkl} S_{ij}(\xi, \theta) S_{kl}(\xi, \theta) - n_j S_{ij}(\xi, \theta) \frac{\partial \zeta_i(\xi, \theta)}{\partial \xi_1} \right) d\bar{s} \quad (26)$$

Here Γ are geometrically scaled closed integration contours BCDE (Fig. 8) with length coordinate s , starting and ending on the crack and passing outside the fracture process zone, $\bar{\Gamma}$ = chosen fixed contour in dimensionless coordinates, with length coordinate \bar{s} ($ds = D d\bar{s}$), n_i = unit normal to the contour (which does not change with scaling), W = strain energy density; $\mathcal{J}(\theta)$ is the dimensionless J-integral. This integral may be expanded in Taylor series, providing

$$\mathcal{J}(\theta) = \mathcal{J}_0 + \mathcal{J}_1 \theta + \mathcal{J}_2 \theta^2 + \dots \quad (27)$$

$$\mathcal{J}_0 = \int_{\bar{\Gamma}} [c_{ijkl} S_{ij}^0 S_{kl}^0 / 2 - n_j S_{ij}^0 \zeta_{i,1}^0] d\bar{s}, \quad (28)$$

$$\mathcal{J}_1 = \int_{\bar{\Gamma}} [c_{ijkl} (S_{ij}^0 S_{kl,\theta}^0 + S_{kl}^0 S_{ij,\theta}^0) / 2 - n_j (S_{ij}^0 \zeta_{i,1\theta}^0 + S_{ij,\theta}^0 \zeta_{i,1}^0)] d\bar{s} \quad (29)$$

Superscript 0 labels the values or fields evaluated for $\theta = 0$ (which is the case of LEFM). Substituting this into (25), truncating the series after the second term, and noting that, at failure, J must be equal to the fracture energy G_f of the material, one gets again the same size effect law as before:

$$\sigma_N = \sqrt{\frac{2EG_f}{[\mathcal{J}_0 + \mathcal{J}_1(c_f/D) + \mathcal{J}_2(c_f/D)^2 + \dots]D}} \approx \frac{Bf'_t}{\sqrt{1 + (D/D_0)}} \quad (30)$$

where $Bf'_t = \sqrt{2EG_f/\mathcal{J}_1c_f}$ and $D_0 = c_f\mathcal{J}_1/\mathcal{J}_0$. The truncation leading to this formula is of course justified only if \mathcal{J} is non-zero and non-negligible, which means that a notch of stress-free crack is assumed to exist at the outset.

The foregoing derivation has been simplified in the sense that the length parameter influencing J has been considered as a known constant. Although this seems a good approximation, one could more generally consider J to depend on c/D instead of c_f/D , where c is a variable crack extension. One could then also introduce a variable fracture resistance in the form of an R -curve, and impose the maximum load condition as the condition of the tangency of the R -curve to the energy release curve, in the same manner as used in equivalent LEFM analysis by Bažant (1996). The size effect law ensuing from such refined analysis is found to be the same.

For the case of LEFM, corresponding to the limit $\theta = c_f/D \rightarrow 0$, the foregoing J-integral analysis (which can be simplified) proves in general that the power law for stress scaling has the exponent $m = -1/2$.

The foregoing derivation can be generalized to the case of fracture with a known residual crack-bridging stress σ_r applied on the crack faces, as considered for compression fracture (Fig. 8). In that case the stress distributions for various sizes are written as

$$\sigma_{ij} = \sigma_N S_{ij}(\xi, \theta) + \sigma_r T_{ij}(\xi, \theta) \quad (31)$$

The J-integral must in this case be generalized by extending its path along the crack surfaces along which the work is non-zero (Fig. 8). As it transpires, the path must begin and end at the points on the crack surfaces that lie at the boundary of the fracture process zone (points A and B in Fig. 1), i.e., the integration path must be ABCDEF because the contribution from the path segments AB and EF along the crack surface is not zero. The subsequent procedure is analogous.

9 Effect of Material Orthotropy

In the case of fiber composites, LEFM must be generalized to take into account the orthotropy of the material. The stress intensity factor of a sharp crack with a negligibly small FPZ may always be written in the form:

$$K_I = \sigma_N \sqrt{\pi D \alpha} F(\alpha) \quad (\alpha = a/D) \quad (32)$$

where σ_N = nominal stress, considered here at maximum load, D = characteristic dimension, a = crack length, α = relative crack length, and $F(\alpha)$ = function characterizing structure geometry and material orthotropy.

The energy release rate \mathcal{G} may be related to K_I using Bao et al.'s (1992) generalization of Irwin's (1958) relation for orthotropic materials:

$$\mathcal{G} = \frac{K_I^2}{\bar{E}} = \frac{D}{\bar{E}} \sigma_N^2 g(\alpha), \quad g(\alpha) = \pi \alpha [F(\alpha)]^2 \quad (33)$$

where $g(\alpha)$ = dimensionless energy release function, characterizing the structure geometry and material orthotropy, and

$$\bar{E} = \frac{1}{Y(\rho)^2} \frac{(E_2/E_1)^{1/4}}{\sqrt{(1+\rho)/2E_1E_2}}, \quad \text{with} \quad \rho = \frac{\sqrt{E_1E_2}}{2G_{12}} - \sqrt{\nu_{12}\nu_{21}} \quad (34)$$

$$Y(\rho) = [1 + 0.1(\rho - 1) - 0.015(\rho - 1)^2 + 0.002(\rho - 1)^3][(\rho + 1)/2]^{-1/4} \quad (35)$$

Subscripts 1 and 2 refer to Cartesian axes $x_1 \equiv x$ and $x_2 \equiv y$; x_2 coincides with the fiber direction; E_1, E_2, G_{12} , and ν_{12} are the orthotropic elastic constants; and parameters E_2/E_1 and ρ characterize the degree of orthotropy. The formula is valid when the crack propagates in the direction x_1 orthogonal to the fibers, but it is used here as an approximation even for propagation directions forming a small angle with x_1 .

For fracture specimens in the form of long notched strip or slender notched beams, function $g(\alpha)$ or $F(\alpha)$ may be taken approximately the same as for isotropic specimens.

A difficulty still unresolved is that the size of the fracture process zone, c_f , in fiber composites depend strongly on the direction of fracture propagation with respect to the fibers. Complex questions remain with regard to the role of pullout and breakage of fibers in the fracture process zone.

10 Kink Bands in Fiber Composites

A kink band, in which axial shear-splitting cracks develop between fibers which undergo microbuckling, is one typical mode of compression failure of composites or laminates with uniaxial fiber reinforcement. This failure mode, whose theory was begun by Rosen (1965) and Argon (1972), was until recently treated by the theory of plasticity, which implies no size effect. Recent experimental and theoretical studies (see Budianski et al. 1997), however, revealed that the kink band propagates side-way like a crack and the stress on the flanks of the band gets reduced to a certain residual value, which is here denoted as σ_Y and can be estimated by the classical plasticity approach of Budianski (1983). The crack-like behavior implies a size effect, which is demonstrated by the latest Bažant et al.'s (1999) laboratory tests of notched carbon-PEEK specimens (Fig. ??); these tests also demonstrated the possibility of a stable growth of a long kink band, which was achieved by rotational restraint at the ends).

There are again two types of size effect, depending on whether P_{max} is reached (i) when the FPZ of the kink band is attached to a smooth surface or (ii) or when there exists either a notch or a long segment of kink band in which the stress has been reduced to σ_Y . Our previous size effect formulae can approximately describe the size effects for these two basic cases; in this case G_f now plays the role of fracture energy of the kink band (area below the stress-contraction curve of the kink band and above the σ_Y value), and c_f the role of the FPZ of the kink band, which is assumed to be approximately constant, governed by material properties.

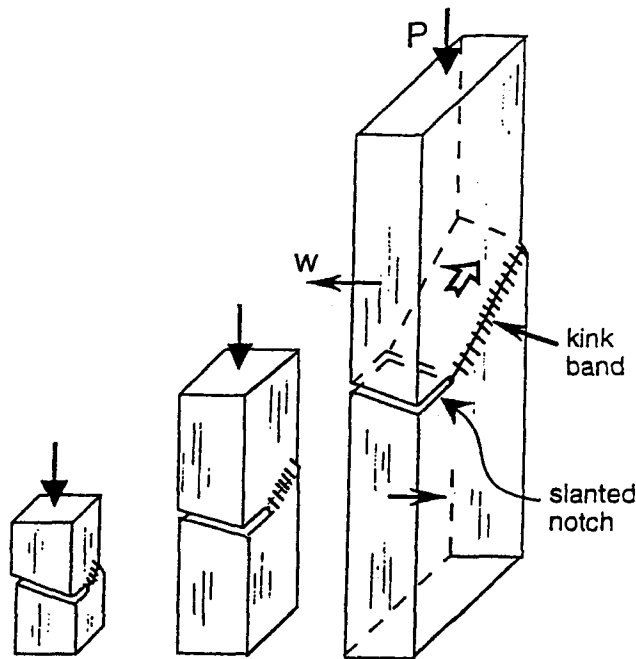


Figure 6: Geometrically similar single-edge notched carbon-PEEK (poly-ether-ether-keton) specimens tested (after Bažant et al. 1999).

The aforementioned carbon-PEEK tests also confirm that case (ii), in which a long kink band grows stably prior to P_{max} , is possible (in those test, this is by virtue of a lateral shift of compression resultant in wide notched prismatic specimens with ends restrained against rotation).

11 Scaling via J-Integral, with Application to Kink Bands in Fiber Composites

11.1 J-Integral Analysis of Size Effect on Kink Band Failures

It is instructive to show now the application of the J-integral to the derivation of the basic scaling properties of kink band failures, as presented in Bažant et al. 1999. This represents the most fundamental approach to fracture. Let us analyze the specimen with unidirectional (axial) fiber reinforcement shown in Fig. 11.1 and 11.1. The kink band has length a which can be long or short compared to the specimen width D taken as the characteristic dimension. The width of the kink band, considered to be small, is denoted as w , and its inclination as β (Fig. 11.1a, 11.1). Although tractable, the bending stiffness of the fibers is neglected, for the sake of simplicity.

The loading is assumed to produce cohesive shear cracks that are parallel to the fibers and have a certain characteristic spacing s . The axial normal stress transmitted across the kink band (band-bridging stress) is denoted as σ (Fig. 11.1). Although Fig. 11.1a depicts an in-plane fiber inclination, the behavior is similar for the out-of-plane fiber inclination in the test specimen used because what matters for the analysis is the reduction of axial stress across the kink band, which is the same for

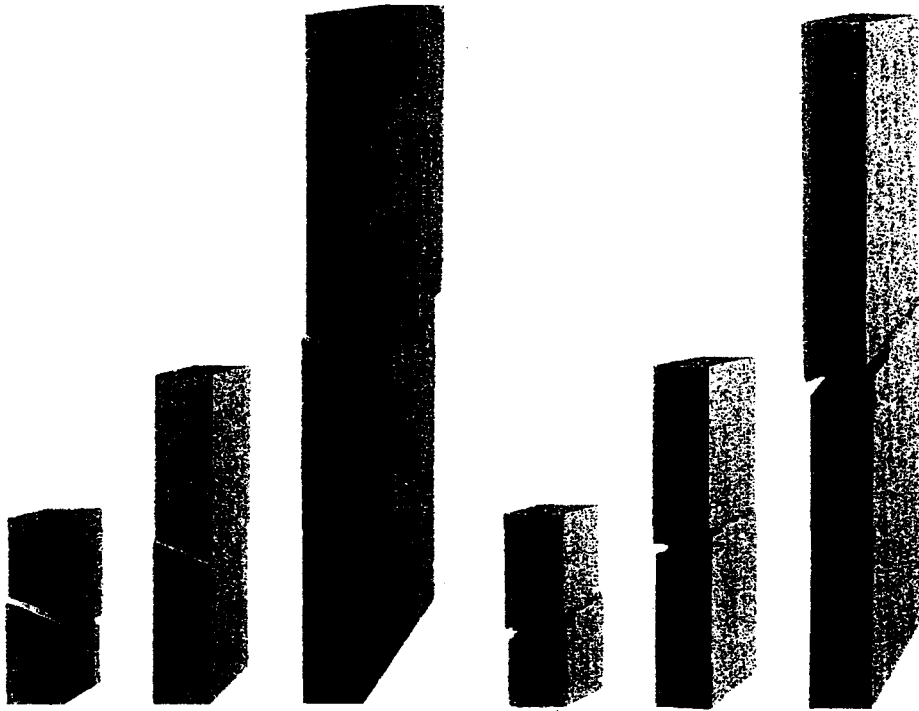


Figure 7: Photo of three of the specimens after the test, showing the out-of-plane kink band (after Bažant et al. 1999).

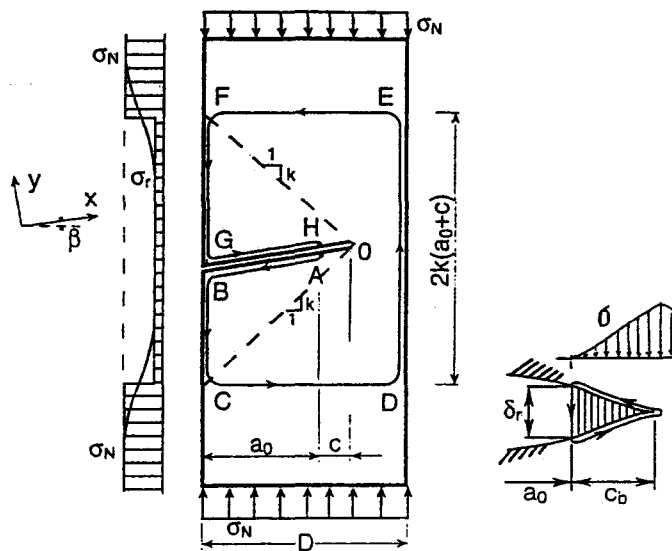


Figure 8: Path of J-integral used in size effect analysis, with energy release (stress relief) zones OFGO, OBCO, and (on the right) fracture process zone of equivalent cohesive crack.

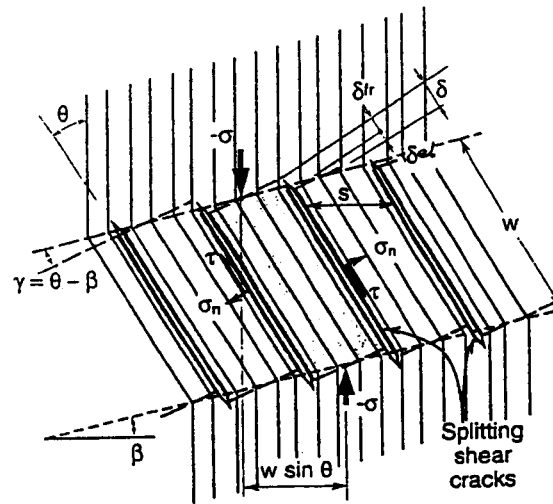


Figure 9: Idealized microbuckling of fibers in the kink band and axial shear cracks.

both cases.

The diagram of the shear stress τ transmitted across the shear cracks versus the slip displacement η_f on these cracks must exhibit post-peak softening (Fig. 11.1 top left). This is confirmed by two important recent experimental findings.

First, Fleck and Shu (1995) placed strain gauges at the flanks of the kink band and, as the kink band grew, observed the strain in the gages to decrease, rather than remain constant (see also Fleck 1997). Second, Moran et al. (1995) recently discovered the phenomenon of band broadening (see also Sutcliffe et al. 1996), which implies that the relative displacement across the band increases as the band grows, and thus indicates that the kink band plays a role similar to a crack (whose opening width grows with the distance from the front and the transmitted stress decreases), rather than to a dislocation line (on which the relative displacement as well as the transmitted stress remains constant).

For the sake of simplicity, the stress-displacement diagram of the axial shear cracks is considered to be bilinear, as shown in Fig. 11.1 (top right) where τ_p = peak stress or shear strength = shear stress parallel to fibers at which the cohesive crack initiates, and τ_r = the residual shear strength, representing the final yield plateau. According to the analysis of mode II slip bands by Palmer and Rice (1973), the area of the diagram above the yield plateau is known to play the role of shear (Mode II) fracture energy, G_f (see the shaded triangle in Fig. 11.1 top left) (the critical value J_{cr} of the J-integral also includes the rectangle below the triangle). The fracture energy of the kink band, that is, the energy dissipated by fracture per unit length of the band, is

$$G_b = G_f w / s \quad (36)$$

11.2 J-integral Calculations

To approximately calculate the energy release due to propagation of the kink band, we use Rice's (1968a) J-integral, for which we consider the rectangular closed path $ABCDEFGH$ shown in Fig.

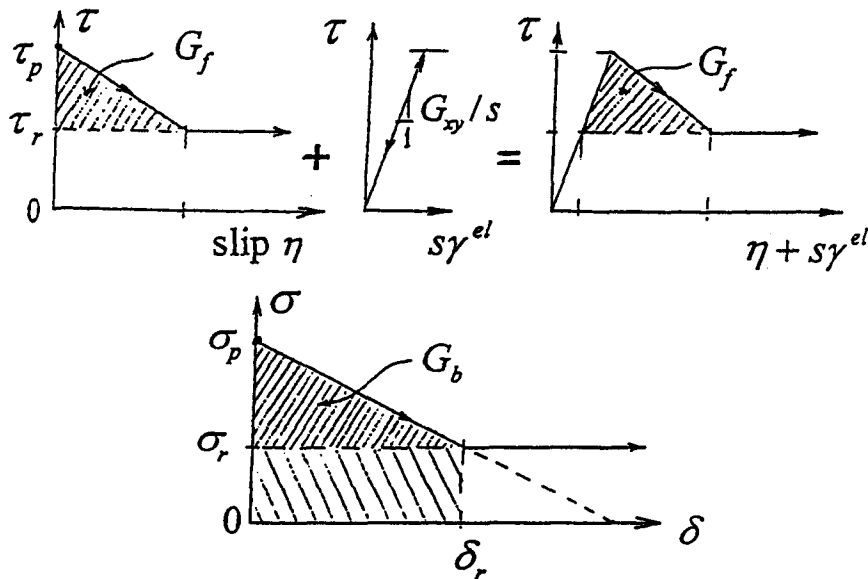


Figure 10: Top left: assumed bilinear diagram of shear stress versus slip displacement on the axial cracks of spacing s , crossing the kink band. Top right: superposition of elastic deformation between the cracks to obtain the diagram of shear stress versus total shear displacement accumulated over distance s between cracks. Bottom: Diagram of the axial normal stress σ versus axial displacement δ across the kink band, and area representing the kink band fracture energy G_b .

11.1b. The start and the end of this path at the crack surfaces must lie at the boundary of the FPZ because the residual stress across the band does work (for Mode II cracks this was shown by Palmer and Rice, 1973). The top, bottom and right sides of this rectangular path, $CDEF$, are sufficiently remote from the crack band for the initially uniform stress state so as to remain undisturbed.

On the left downward sides of the rectangular path, FG and BC , the distribution of the axial stress has some curved profile sketched on the left of Fig. 11.1b. The precise shape of this profile is not important but it is important that asymptotically, for large sizes $D \gg w$, the profiles must become geometrically similar. This observation is the basic idea of the asymptotic size effect analysis via the J-integral.

For the sake of simplicity, we may replace this profile by the stepped piece-wise constant profile shown, in which the stress drops abruptly from the initial stress σ_N to the residual stress σ_r which is transmitted across the band after the band contracts sufficiently. An important point again is that, for large enough geometrically similar specimens ($D \gg w$), the locations of the stress steps in this replacement profile must also be similar, that is, points F and C , must lie on inclined rays of a certain constant slope k shown dashed in Fig. 11.1b. These rays may be imagined to emanate from the tip of the equivalent crack of length $a = a_0 + c_b$ (Fig. 11.1b) where c_b characterizes the length of the FPZ of the kink band and represents approximately the distance from the center of the FPZ of kink band to the point where the stress is reduced to its residual value σ_r (Fig. 11.1 top; the length of the FPZ is about $2c_b$). Slope k depends on the structure geometry and on the orthotropic elastic constants.

The area between these rays and the kink band roughly represents the zone of stress relief caused by the drop of axial stress transmitted by the kink band. The strain energy contained within this area is released and is dissipated by the axial shear cracks forming at the front of the kink band. Noting that this area, and thus the energy release, increases in proportion to D^2 , while the energy dissipated at the kink band front increases linearly with D , one immediately concludes that there

must be size effect.

The zone at kink band front in which the axial shear cracks are forming represents the FPZ of the kink band. Its length c_0 may be regarded as a material property, almost independent of the specimen dimensions and geometry. It may be considered to be of the same order of magnitude as the width w . Throughout this zone, the fiber inclination increases from the initial misalignment angle $\bar{\varphi}$ up to the value $\bar{\varphi} + \varphi$ corresponding to the residual cracks. To make test evaluation simple, the specimens must be notched and the FPZ at maximum load must still be attached to the notch (i.e. $c = c_0$).

Referring to the sketch in Fig. 11.1b, the crack band of length $a_0 + c_f$ is approximately equivalent to a mode I crack whose faces are imagined to interpenetrate. The length of this crack is $a_0 + c$ where $c = c_f + (w/2k)$, which may again be assumed to be approximately a constant when the size is varied. Consequently, the height FC of the rectangular path in Fig. 11.1b is approximately $2k(a_0 + c)$, as labeled in the figure.

As a result of these considerations, the first part of the J-integral may be approximately expressed as follows (Bazant et al. 1999):

$$\oint \bar{W} dy = 2k(a_0 + c) \left(\frac{\sigma_N^2}{2E_y} - \frac{\sigma_r^2}{2E_y} \right) \quad (37)$$

in which \bar{W} = strain energy density, and y = coordinate normal to the direction of propagation (Fig. 11.1b), and E_y = effective elastic modulus of the orthotropic fiber composite in the fiber direction y (with different values for plane strain and plane stress). In (37) we have considered that the parts of the integral over the horizontal segments are 0, and that the stress on the vertical segment DE may be assumed undisturbed by the kink band, i.e., equal to σ_N . The portions of the integral over the crack surface segments GH and AB are, likewise, 0.

The second part of the J-integral may be calculated in a similar manner as that introduced by Palmer and Rice (1973) for the propagation of Mode II shear fracture with residual friction;

$$\begin{aligned} \oint \bar{\sigma} \cdot \frac{\partial \bar{u}}{\partial x} ds &= \int_{AB} \sigma_r \frac{d}{dx} \left[\frac{1}{2} \delta(x) \right] dx - \int_{GH} \sigma_r \frac{d}{dx} \left[\frac{1}{2} \delta(x) \right] dx \\ &= \int_{x=0}^{a_0} \sigma_r d\delta(x) = \sigma_r \int_{x=0}^{a_0} d\delta(x) = \sigma_r \delta_{BC} \end{aligned} \quad (38)$$

in which $\bar{\sigma}$ = stress vector acting from the outside on the domain enclosed by the path, \bar{u} = displacement vector, s = length coordinate along the path, δ = relative displacement across the band, and δ_{BC} = relative displacement between points B and G . That displacement can be estimated as the difference between the changes of length \overline{ED} and length \overline{FC} ;

$$\delta_{BC} = \Delta \overline{ED} - (\Delta \overline{FG} + \Delta \overline{BC}) \quad (39)$$

$$= 2k(a_0 + c) \frac{\sigma_N}{E_y} - 2k(a_0 + c) \frac{\sigma_r}{E_y} = 2k(a_0 + c) \frac{\sigma_N - \sigma_r}{E_y} \quad (40)$$

Now the J-integral may be readily evaluated as follows:

$$\begin{aligned} J &= \oint \left(\bar{W} dy - \bar{\sigma} \cdot \frac{\partial \bar{u}}{\partial x} ds \right) = \frac{k}{E_y} (a_0 + c) \left[\sigma_N^2 - \sigma_r^2 - 2(\sigma_N - \sigma_r)\sigma_r \right] \\ &= \frac{k}{E_y} (a_0 + c) (\sigma_N - \sigma_r)^2 \end{aligned} \quad (41)$$

The energy consumed may be calculated again with the help of the J-integral. Similar to Rice (1968b) and Palmer and Rice (1973), the integration path that runs along the equivalent crack surface and around the crack tip (Fig. 11.1c) may be used;

$$J_{cr} = \oint \bar{\sigma} \cdot \frac{\partial \bar{u}}{\partial x} dx \quad (42)$$

This represents the critical value, J_{cr} , of the J-integral required for propagation. This critical value may be subdivided into two terms:

$$J_{cr} = G_b + \sigma_r \delta_r \quad (43)$$

where G_b is the fracture energy, i.e., the energy required to produce the axial shear cracks across the kink band, and $\sigma_r \delta_r$, represents the plastic work that is done by the residual stresses σ_r within the FPZ of the kink band and is leaving the FPZ in its wake. This work corresponds in Fig. 11.1 (top left) to the shaded rectangle lying under the shaded triangle. Following the way shown by Rice (1968b) and Palmer and Rice (1973) for shear bands, J_{cr} may be evaluated (Fig. 11.1c) as follows:

$$\begin{aligned} J_{cr} &= \oint \bar{\sigma} \cdot \frac{\partial \bar{u}}{\partial x} dx = - \int_{x=a_0}^{a_0+c} f[\delta(x)] \frac{d}{dx} \left[\frac{1}{2} \delta(x) \right] dx + \int_{x=a_0+c}^{a_0} f[\delta(x)] \frac{d}{dx} \left[\frac{1}{2} \delta(x) \right] dx \\ &= - \int_{x=a_0}^{a_0+c} f[\delta(x)] \frac{d\delta(x)}{dx} dx = \int_0^{\delta_r} f[\delta(x)] d\delta(x) \end{aligned} \quad (44)$$

(Bažant et al. 1999). This means that J_{cr} represents the sum of the shaded triangle and shaded rectangle in the stress-displacement diagram of Fig. 11.1 (top left). Therefore, according to (43), fracture energy G_b is represented by the area under the descending stress-displacement curve and above the horizontal line for the residual stress.

11.3 Case of Long Kink Band

Setting (41) equal to (43), and solving for the nominal strength σ_N of the specimen, we obtain (Bažant et al. 1999):

$$\sigma_N = \sigma_R + \sqrt{\frac{E_y(G_b + \sigma_r \delta_r)/kc}{1 + D/D_0}} = \sigma_R + \frac{\sigma_0}{\sqrt{1 + D/D_0}} \quad (45)$$

in which

$$D_0 = \frac{c}{\alpha_0}, \quad \sigma_0 = \sqrt{\frac{E_y(G_b + \sigma_r \delta_r)}{kc}}, \quad \alpha_0 = \frac{a_0}{D}, \quad \sigma_R = \sigma_r \quad (46)$$

(for other geometries, σ_R need not be equal to σ_r). The resulting formula (45) has the same form as that proposed by Bažant (1987) for the general case of quasibrittle failures with a residual plastic mechanism, and subsequently verified for several applications to concrete structure. This formula is valid when a long enough kink band transmitting constant residual stress σ_r develops in a stable manner before the maximum load is reached. Because of σ_r , such stable propagation can happen even in specimens of positive geometry (i.e., for increasing $g(\alpha)$). Stable propagation is helped by rotational restraint of specimen ends.

The energy consumed may be calculated again with the help of the J-integral. Similar to Rice (1968b) and Palmer and Rice (1973), the integration path that runs along the equivalent crack surface and around the crack tip (Fig. 11.1c) may be used;

$$J_{cr} = \oint \bar{\sigma} \cdot \frac{\partial \bar{u}}{\partial x} dx \quad (42)$$

This represents the critical value, J_{cr} , of the J-integral required for propagation. This critical value may be subdivided into two terms:

$$J_{cr} = G_b + \sigma_r \delta_r \quad (43)$$

where G_b is the fracture energy, i.e., the energy required to produce the axial shear cracks across the kink band, and $\sigma_r \delta_r$, represents the plastic work that is done by the residual stresses σ_r within the FPZ of the kink band and is leaving the FPZ in its wake. This work corresponds in Fig. 11.1 (top left) to the shaded rectangle lying under the shaded triangle. Following the way shown by Rice (1968b) and Palmer and Rice (1973) for shear bands, J_{cr} may be evaluated (Fig. 11.1c) as follows:

$$\begin{aligned} J_{cr} &= \oint \bar{\sigma} \cdot \frac{\partial \bar{u}}{\partial x} dx = - \int_{x=a_0}^{a_0+c} f[\delta(x)] \frac{d}{dx} \left[\frac{1}{2} \delta(x) \right] dx + \int_{x=a_0+c}^{a_0} f[\delta(x)] \frac{d}{dx} \left[\frac{1}{2} \delta(x) \right] dx \\ &= - \int_{x=a_0}^{a_0+c} f[\delta(x)] \frac{d\delta(x)}{dx} dx = \int_0^{\delta_r} f[\delta(x)] d\delta(x) \end{aligned} \quad (44)$$

(Bažant et al. 1999). This means that J_{cr} represents the sum of the shaded triangle and shaded rectangle in the stress-displacement diagram of Fig. 11.1 (top left). Therefore, according to (43), fracture energy G_b is represented by the area under the descending stress-displacement curve and above the horizontal line for the residual stress.

11.3 Case of Long Kink Band

Setting (41) equal to (43), and solving for the nominal strength σ_N of the specimen, we obtain (Bažant et al. 1999):

$$\sigma_N = \sigma_R + \sqrt{\frac{E_y(G_b + \sigma_r \delta_r)/kc}{1 + D/D_0}} = \sigma_R + \frac{\sigma_0}{\sqrt{1 + D/D_0}} \quad (45)$$

in which

$$D_0 = \frac{c}{\alpha_0}, \quad \sigma_0 = \sqrt{\frac{E_y(G_b + \sigma_r \delta_r)}{kc}}, \quad \alpha_0 = \frac{a_0}{D}, \quad \sigma_R = \sigma_r \quad (46)$$

(for other geometries, σ_R need not be equal to σ_r). The resulting formula (45) has the same form as that proposed by Bažant (1987) for the general case of quasibrittle failures with a residual plastic mechanism, and subsequently verified for several applications to concrete structure. This formula is valid when a long enough kink band transmitting constant residual stress σ_r develops in a stable manner before the maximum load is reached. Because of σ_r , such stable propagation can happen even in specimens of positive geometry (i.e., for increasing $g(\alpha)$). Stable propagation is helped by rotational restraint of specimen ends.

11.4 Failure at the Start of Kink Band from a Notch or Stress-Free Crack

In the case of notched test specimens (of suitable geometry), the maximum load is achieved while the FPZ of the kink band is still attached to the notch. Except for the sign of the band-bridging stresses, the situation is analogous to tensile fracture of notched specimens. From experiments on concrete as well as analytical studies based on the cohesive crack model, it is known that only a short initial portion of the softening stress-displacement curve of the cohesive crack comes into play. It is only the initial downward slope of this curve which matters for the maximum load (the tail of the postpeak load-deflection diagram, of course, depends on the entire stress-displacement curve of the cohesive crack); see Bažant and Li (1995) or Bažant and Planas (1998).

A similar situation must be expected for kink bands in notched specimens. Since the shape of the softening stress displacement curve of the cohesive crack model is irrelevant for the maximum load, except for the initial downward slope of the curve, the maximum load must be the same as that for a linear stress-displacement diagram, shown by the descending dashed straight line shown in Fig. 11.1 (bottom).

It follows that in this case the residual stress σ_r should be disregarded and the fracture energy G_B that mathematically governs the kink band growth at maximum load of a notched specimen corresponds to the entire area under the extended descending straight line in Fig. 11.1. Obviously, $G_B > G_b$ if $\sigma_r > 0$. Consequently, setting $\delta_r = 0$ in (46) and replacing G_b by G_B , we have the size effect law:

$$\sigma_N = \frac{\sigma_0}{\sqrt{1 + D/D_0}} \quad (47)$$

with

$$D_0 = \frac{c_0}{\alpha_0}, \quad \sigma_0 = \sqrt{\frac{E_y G_B}{k c_0}}, \quad c_0 = c_b + \frac{w}{2k} \quad (48)$$

(Bažant et al. 1999). This coincides with the approximate size effect law proposed in Bažant (1983, 1984); Fig. 11.4 (left, for $\sigma_R = 0$).

Based on the experience with other materials, the length (at maximum load) of the crack band up to the beginning of the FPZ, a_0 , may often be considered to be roughly proportional to the specimen size D , within a certain range of sizes. In other words, the ratio D/a_0 at maximum load of geometrically similar structures is often approximately constant. So is the value of D_0 in (47), provided that the specimens are geometrically similar.

Analogous results are obtained via equivalent LEFM (Bažant et al. 1999). This approach relies on some stronger simplifications but has the advantage that effect of structure geometry is also captured.

11.5 Comparison with Size Effect Tests of Kink Band Failures

To demonstrate the existence of a size effect in kink band failure and justify the present analysis, tests of relatively large carbon fiber-PEEK specimens of three different sizes (Fig. 11.1) have been carried out at Northwestern University (Bažant et al. 1999). Slanting of the notches was found to achieve that no axial shear-splitting would precede or accompany the kink band growth (Fig. 11.1).

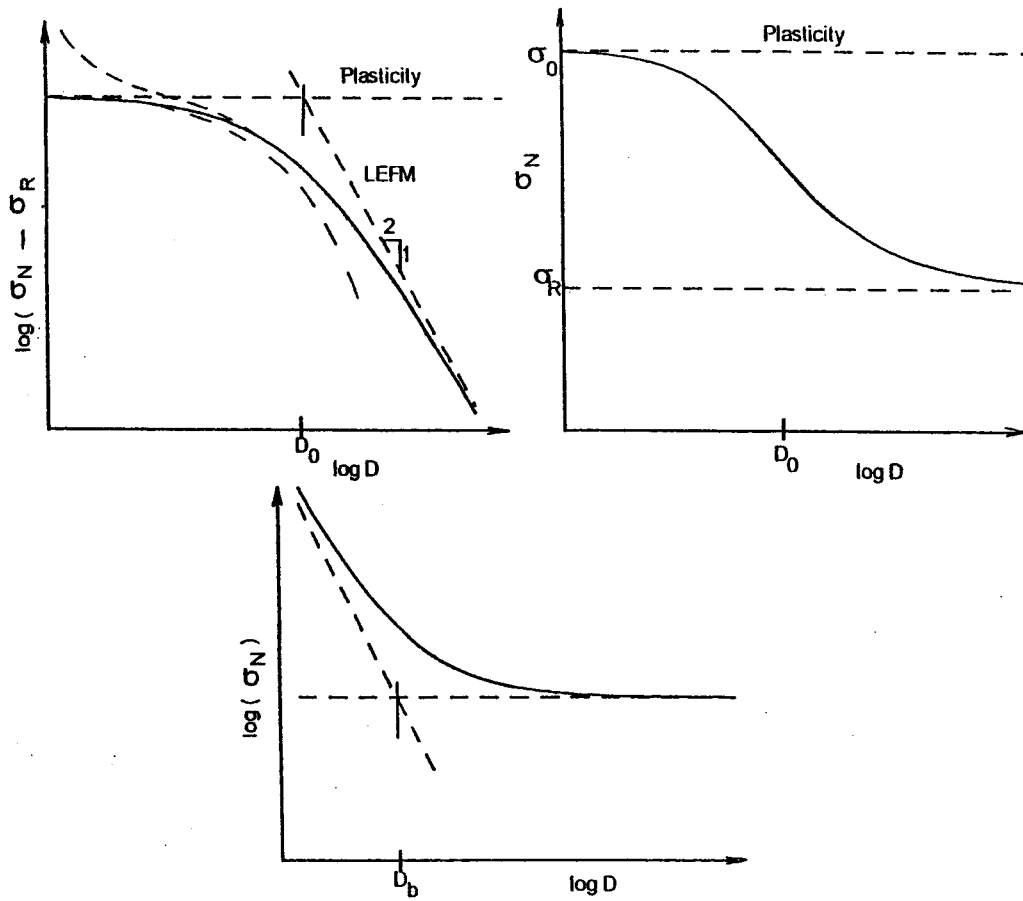


Figure 11: Top left: Size effect law (solid curve) for specimens with a long kink band or notch, and asymptotic formulas (dashed curves). Top right: Same but with σ_N instead of $\log \sigma_N$ as the ordinate; curves). Bottom: Size effect law when P_{max} occurs at kink band initiation.

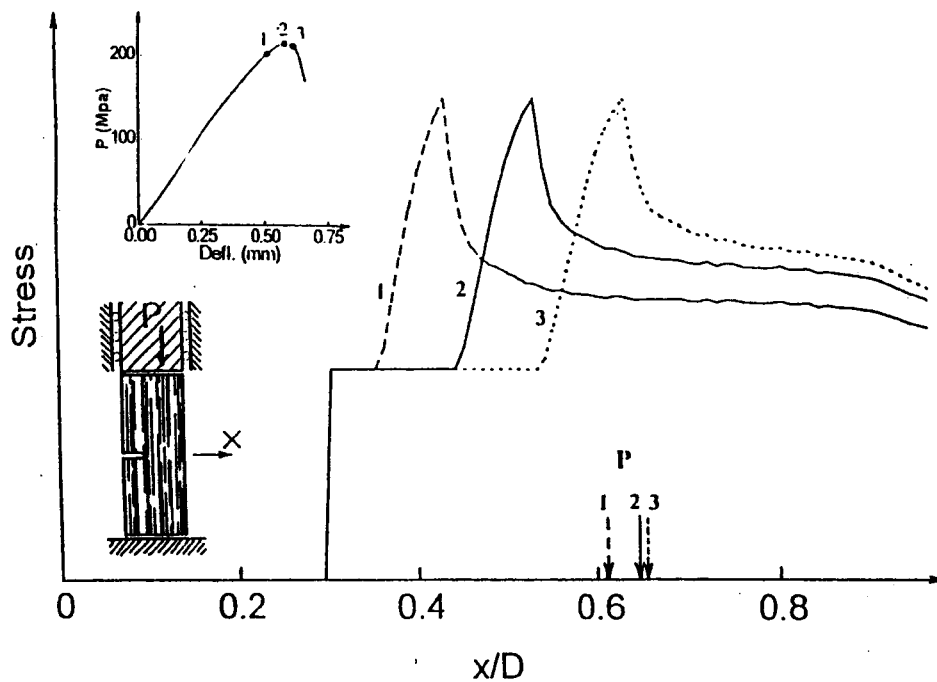


Figure 12: Stress profiles across the ligament of the carbon-PEEK specimens before, at and after the maximum load (note the shift of the compression resultant P , which makes a stable kink band growth possible) (after Bažant et al. 1999).

Rigid restraint against rotation at the ends made it possible for the kink band to growth stably for a considerable distance before attaining the maximum compression load. Attainment of this goal was verified experimentally and is was also demonstrated theoretically by the subsequent stress profiles along the kink band calculated with the cohesive crack model (Fig. 11.5).

The results of individual tests are shown in Fig. 11.5. Despite high scatter, which is probably inevitable in the case of fiber composites, one can see that the present theory does not disagree with the test results (Bažant et al. 1999).

The present fracture theory exhibiting size effect may also be verified by comparison with the test results of Soutis, Curtis and Fleck (1993). They used rectangular prisms with circular holes. Although they did not vary the specimen size, they varied the hole size, which represents a combination of size effect and shape effect. Thanks to the fact that the formulation based on the equivalent LEFM captures also the shape effect, the asymptotic formula derived in Bažant et al. (1999) could be used to fit the data. The comparison showed that the theory exhibiting size effect allows much better fits than a theory lacking the size effect (Fig. 11.5).

The results make it clear that the present theories of kink-band failure, which are based on plasticity or strength criteria, are adequate only for small structural parts. For large one, the size effect must be taken into account.

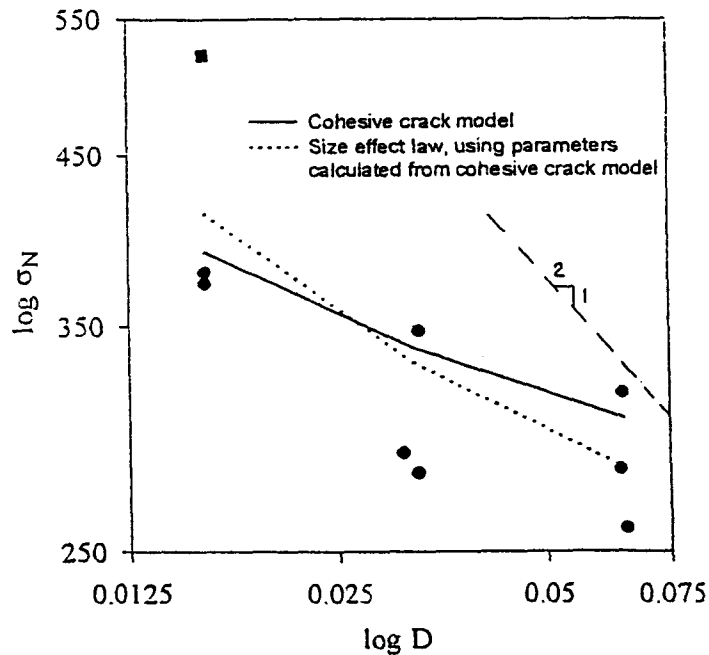


Figure 13: Optimum fits of kink band tests on PEEK with numerical analysis by the cohesive crack model and by the size effect formulae modified for dissimilar locations of the axial load resultant (after Bažant et al. 1999).

12 Remarks on Size Effect in Sandwich Plates and Rigid Foams

The course also featured a discussion of failure of sandwich plates with fiber laminate skins and polymeric foam core. This subject will not be presented here since it was presented in Bažant and Brocca (2000) and Brocca and Bažant (2001). Suffice to say that: (1) Finite element analysis with a recently developed microplane model for closed-cell cellular materials shows that size effect should exist, and (2) recent tests of notched specimens of vinyl foam used for sandwich cores reveal a strong deterministic size effect, closely approaching LEFM; see Fig. 15.

13 Closing Comments

Although the recent progress has been significant, the understanding of the scaling problems of solid mechanics is nevertheless far from complete, especially for fiber composites and sandwich structures. Mastering the size effect that bridges different behaviors on adjacent scales in the microstructure of material will be contingent upon the development of realistic constitutive and fracture models that possess a material length (or characteristic length). The theory of nonlocal continuum damage will have to move beyond the present phenomenological approach and take into account the directional and tensorial interactions between the effects causing nonlocality. A statistical description of such interactions will have to be developed, especially for composites. Discrete element models of the microstructure of fracturing or damaging materials will be needed to shed more light on the mechanics of what is actually happening inside the material and separate the important processes from the

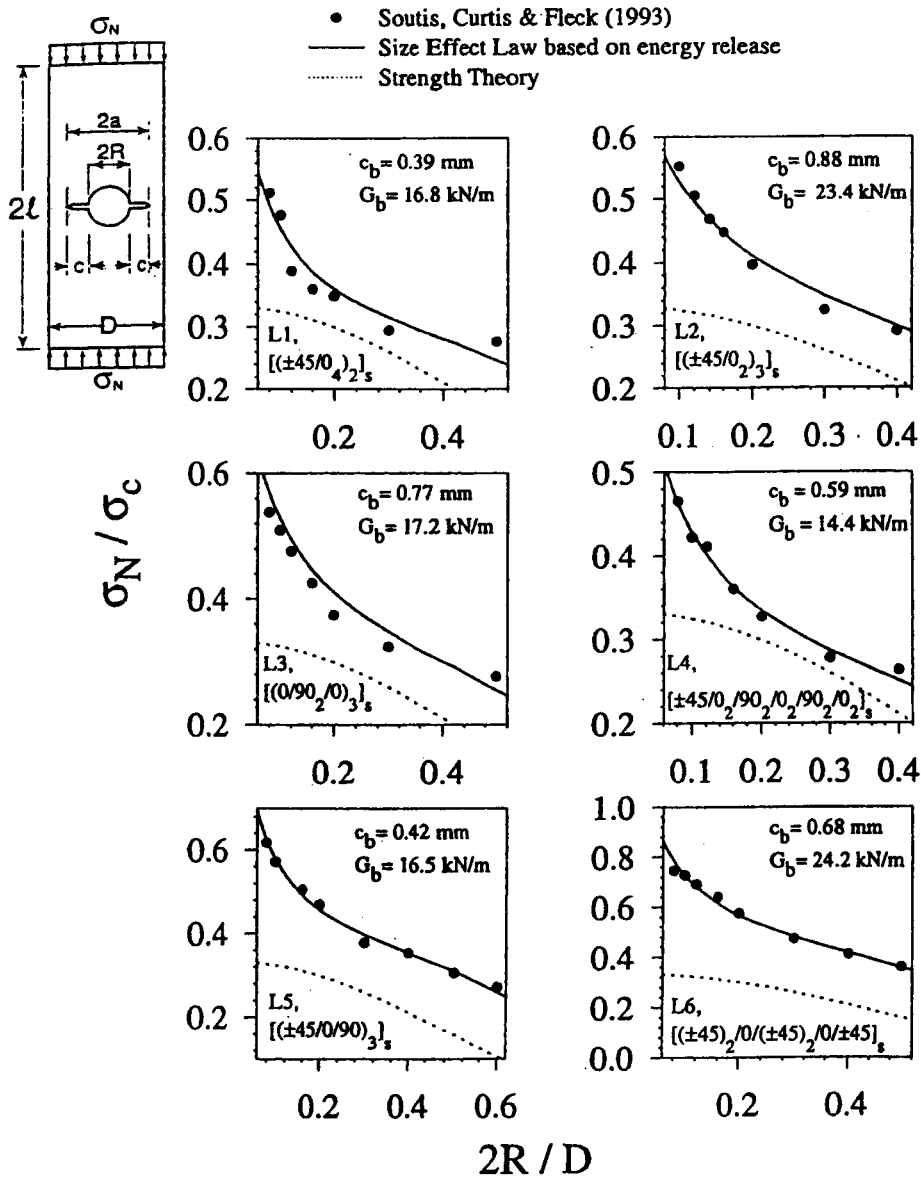


Figure 14: Soutis, Curtis and Fleck's (1993) test results for quasi-isotropic and orthotropic carbon–epoxy laminates of six different layups, with holes of various radii R (data points) and constant width D . Solid curves: optimum fits by size effect law. Dashed curves: predictions of strength theory exhibiting no size effect (after Bažant et al. 1999).

Size Effect on Tensile Fracture of Divinycell H100 Foam

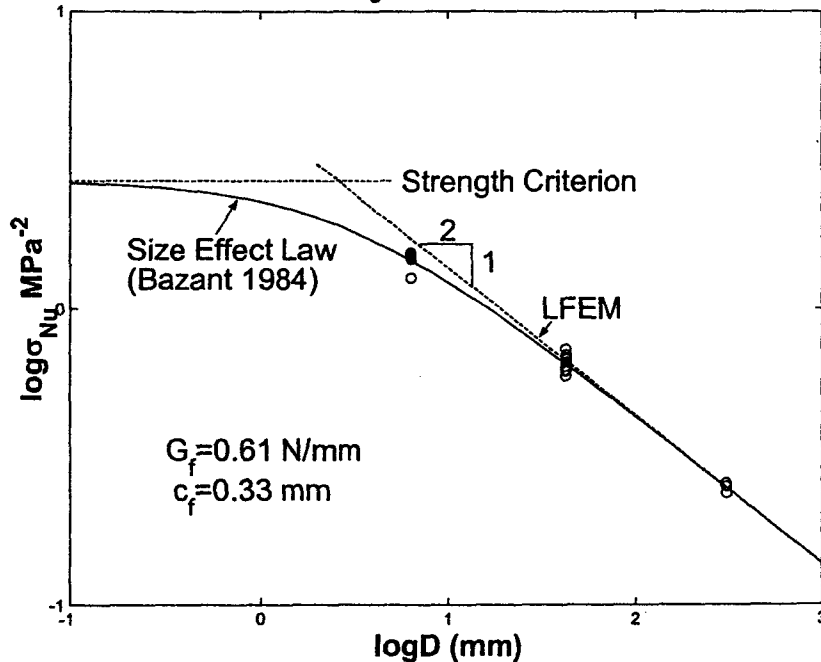


Figure 15: Size effect observed at Northwestern University (by Y. Zhou and Z.P. Bažant) in tests of notched specimens of Divinycell 100 foam.

secondary ones.

Acknowledgment: Preparation of the present article was partially supported by the Office of Naval Research under Grant N00014-91-J-1109 to Northwestern University, monitored by Dr. Yapa D.S. Rajapakse.

References

- Argon, A.S. (1972). "Fracture of composites." *Treatise of Materials Science and Technology*, Vol. 1, p. 79, Academic Press, New York.
- Bao, G., Ho, S., Suo, Z. and Fan, B. (1992). "The role of material orthotropy in fracture specimens for composites." *Int. J. Solid Structures*, 29(9), 1105-1116.
- Barenblatt, G.I. (1959). "The formation of equilibrium cracks during brittle fracture. General ideas and hypothesis, axially symmetric cracks." *Prikl. Mat. Mekh.* 23 (3), 434-444.
- Barenblatt, G.I. (1962). "The mathematical theory of equilibrium cracks in brittle fracture", *Advanced Appl. Mech.* 7, 55-129.
- Bažant, Z.P. (1976). "Instability, ductility, and size effect in strain-softening concrete." *J. Engrg. Mech. Div., Am. Soc. Civil Engrs.*, 102, EM2, 331-344; disc. 103, 357-358, 775-777, 104, 501-502.
- Bažant, Z.P. (1984). "Size effect in blunt fracture: Concrete, rock, metal." *J. of Engrg. Mechanics*, ASCE, 110, 518-535."
- Bažant, Z.P. (1987). "Fracture energy of heterogeneous material and similitude." Preprints, SEM-RILEM *Int. Conf. on Fracture of Concrete and Rock* (held in Houston, Texas, June 1987), ed. by S.P. Shah and S.E. Swartz, publ. by SEM (Soc. for Exper. Mech.) 390-402.
- Bažant, Z.P. (1993). "Scaling laws in mechanics of failure." *J. of Engrg. Mech.*, ASCE, 119 (9), 1828-1844.

- Bažant, Z.P. (1998). "Size effect in tensile and compression fracture of concrete structures: computational modeling and design." *Fracture Mechanics of Concrete Structures* (3rd Int. Conf., FraMCoS-3, held in Gifu, Japan), H. Mihashi and K. Rokugo, eds., Aedificatio Publishers, Freiburg, Germany, 1905–1922.
- Bažant, Z.P., Editor (1992). *Fracture Mechanics of Concrete Structures*, Proc., First Intern. Conf. (FraMCoS-1), held in Breckenridge, Colorado, June 1–5, Elsevier, London (1040 pp.).
- Bažant, Z.P. (1992). "Large-scale thermal bending fracture of sea ice plates." *J. of Geophysical Research*, 97 (C11), 17,739–17,751.
- Bažant, Z.P. (1993). "Scaling Laws in Mechanics of Failure." *J. of Engrg. Mech., ASCE*, 119 (9), 1828–1844.
- Bažant, Z.P. (1997a). "Fracturing truss model: Size effect in shear failure of reinforced concrete." *J. of Engrg. Mechanics ASCE* 123 (12), 1276–1288.
- Bažant, Z.P. (1997b). "Scaling of quasibrittle fracture: Asymptotic analysis." *Int. J. of Fracture* 83 (1), 19–40.
- Bažant, Z.P. (1997c). "Scaling of quasibrittle fracture: Hypotheses of invasive and lacunar fractality, their critique and Weibull connection." *Int. J. of Fracture* 83 (1), 41–65.
- Bažant, Z.P. (1999). "Structural stability." *International Journal of Solids and Structures* 37 (200), 55–67; special issue of invited review articles on *Solid Mechanics* edited by G.J. Dvorak for U.S. Nat. Comm. on Theor. and Appl. Mech., publ. as a book by Elsevier Science, Ltd.
- Bažant, Z.P. (1999). "Size effect on structural strength: a review." *Archives of Applied Mechanics* (Ingenieur-Archiv, Springer Verlag) 69, 703–725.
- Bažant, Z.P. (2001). "Scaling of structural strength." Hermes Science Publications, Oxford and Paris.
- Bažant, Z.P., and Cedolin, L. (1991). *Stability of Structures: Elastic, Inelastic, Fracture and Damage Theories* (textbook and reference volume). Oxford University Press, New York, 1991.
- Bažant, Z.P., and Chen, E.-P. (1997). "Scaling of structural failure." *Applied Mechanics Reviews ASME* 50 (10), 593–627.
- Bažant, Z.P., Daniel, I.M., and Li, Zhengzhi (1996). "Size effect and fracture characteristics of composite laminates." *ASME J. of Engrg. Materials and Technology* 118 (3), 317–324.
- Bažant, Z.P., and Kazemi, M.T. (1990). "Size effect in fracture of ceramics and its use to determine fracture energy and effective process zone length." *J. of American Ceramic Society* 73 (7), 1841–1853.
- Bažant, Z.P., and Kazemi, M.T. (1991). "Size effect on diagonal shear failure of beams without stirrups." *ACI Structural Journal* 88 (3), 268–276.
- Bažant, Z.P., Kim, J.-J.H., Daniel, I.M., Becq-Giraudon, E., and Zi, G. (1999). "Size effect on compression strength of fiber composites failing by kink band propagation." *Int. J. of Fracture* (Special Issue on *Fracture Scaling*, ed. by Z.P. Bažant and Y.D.S. Rajapakse), Vol. (June) in press.
- Bažant, Z.P., Kim, J.-J.H., Kim, Daniel, I.M., Becq-Giraudon, E., and Li, Goangseup (1999). "Size effect on compression strength of fiber composites failing by kink band propagation." *Int. J. of Fracture* 95, 103–141 (special issue on *Fracture Scaling*, Z.P. Bažant and Y.D.S. Rajapakse, eds.).
- Bažant, Z.P., and Li, Yuan-Neng (1995). "Stability of cohesive crack model: Part I—Energy principles." *Trans. ASME, J. of Applied Mechanics* 62, 959–964; "Part II—Eigenvalue analysis of size effect on strength and ductility of structures," *ibid.* 62, 965–969.
- Bažant Z.P., and Oh B.-H. (1983). "Crack band theory for fracture of concrete." *Materials and Structures* (RILEM, Paris), 16, 155–177.
- Bažant Z.P. and Pfeiffer, P.A. (1987). "Determination of fracture energy from size effect and brittleness number." *ACI Materials Jour.*, 84, 463–480.
- Bažant, Z.P., and Planas, J. (1998). *Fracture and Size Effect in Concrete and Other Quasibrittle Materials*. CRC Press, Boca Raton, Florida.
- Bažant, Z.P., and Pfeiffer, P.A. (1987), "Determination of fracture energy from size effect and brittleness number." *ACI Materials Jour.*, 84, 463–480.
- Bažant, Z.P. and Xi, Y. (1991). "Statistical size effect in quasi-brittle structures: II. Nonlocal theory." *ASCE J. of Engineering Mechanics* 117 (11), 2623–2640.
- Beremin, F.M. (1983). "A local criterion for cleavage fracture of a nuclear pressure vessel steel." *Metallurgy Transactions A*, 14, 2277–2287.

- Bhat, S.U. (1990). "Modeling of size effect in ice mechanics using fractal concepts", *Journal of Offshore Mechanics and Arctic Engineering* 112, 370–376.
- Budiansky, B. (1983). "Micromechanics." *Computers and Structures* 16 (No. 1–4), 3–12.
- Budiansky, B., Fleck, N.A., and Amazigo, J.C. (1997). "On kink-band propagation in fiber composites." *J. Mech. Phys. Solids* 46 (9), 1637–1635.
- Carpinteri, A. (1986). *Mechanical damage and crack growth in concrete*. Martinus Nijhoff Publ.—Kluwer, Dordrecht–Boston.
- Carpinteri, A. (1989). "Decrease of apparent tensile and bending strength with specimen size: Two different explanations based on fracture mechanics." *Int. J. Solids Struct.*, 25(4), 407–429.
- Carpinteri, A. (1994a). "Fractal nature of material microstructure and size effects on apparent mechanical properties." *Mechanics of Materials* 18 89–101.
- Carpinteri, A. (1994b). "Scaling laws and renormalization groups for strength and toughness of disordered materials." *International Journal of Solids and Structures* 31, 291–302.
- Carpinteri, A., Chiaia, B., and Ferro, G. (1994). "Multifractal scaling law for the nominal strength variation of concrete structures," in *Size effect in concrete structures* (Proc., Japan Concrete Institute International Workshop, held in Sendai, Japan, 1993), ed. by M. Mihashi, H. Okamura and Z.P. Bažant, E & FN Spon, London–New York (1994) 193–206.
- Carpinteri, A. and Chiaia, B. (1995). in *Fracture Mechanics of Concrete Structures* (Proceedings of FraMCoS-2, held at E.T.H., Zürich), ed. by F.H. Wittmann, Aedificatio Publishers, Freiburg, 581–596.
- Carter, B.C. (1992). "Size and stress gradient effects on fracture around cavities." *Rock Mech. and Rock Engng.* (Springer) 25(3), 167–186.
- Carter, B.C., Lajtai, E.Z., and Yuan, Y. (1992). "Tensile fracture from circular cavities loaded in compression." *Int. J. of Fracture*, 57, 221–236.
- Červenka, V., and Pukl, R. (1994). "SBETA analysis of size effect in concrete structures." In *Size Effect in Concrete Structure*, H. Mihashi, H. Okamura and Z.P. Bažant, Eds., E & FN Spon, London, 323–333.
- da Vinci, L. (1500's)—see *The Notebooks of Leonardo da Vinci* (1945), Edward McCurdy, London (p. 546); and *Les Manuscrits de Léonard de Vinci*, transl. in French by C. Ravaisson-Mollien, Institut de France (1881–91), Vol. 3.
- Dempsey, J.P., Adamson, R.M., and Mulmule, S.V. (1995a). "Large-scale in-situ fracture of ice." Vol. 1 (Proc., 2nd Int. Conf. on Fracture Mech. of Concrete Structures (FraMCoS-2), held at ETH, Zürich), ed. by F.H. Wittmann, Aedificatio Publishers, Freiburg, Germany (1995) 575–684.
- Dempsey, J.P., Adamson, R.M., and Mulmule, S.V. (1999b). "Scale effects on the *in situ* tensile strength and fracture of ice: Part II: First-year sea ice at Resolute, N.W.T." *Int. J. of Fracture* 95, 346–378 (special issue on Fracture Scaling, ed. by Z.P. Bažant and Y.D.S. Rajapakse).
- Dempsey, J.P., Slepian, L.I., and Shekhtman, I.I. (1995b). "Radial cracking with closure." *Int. J. of Fracture*, 73 (3), 233–261.
- Dugdale, D.S. (1960). "Yielding of steel sheets containing slits." *J. of Mech. and Phys. of Solids* 8, 100–108.
- Evans, A.G. (1978). "A general approach for the statistical analysis of multiaxial fracture." *J. of the Am. Ceramic Soc.* 61, 302–308.
- Fréchet, M. (1927). "Sur la loi de probabilité de l' écart maximum." *Ann. Soc. Polon. Math.* 6, p. 93.
- Fisher, R.A. and Tippett, L.H.C. (1928). "Limiting forms of the frequency distribution of the largest and smallest member of a sample." *Proc., Cambridge Philosophical Society* 24, 180–190.
- Frankenstein, E.G. (1963). "Load test data for lake ice sheet." *Technical Report 89*, U.S. Army Cold Regions Research and Engineering Laboratory, Hanover, New Hampshire.
- Frankenstein, E.G. (1966). "Strength of ice sheets." *Proc., Conf. on Ice Pressures against Struct.; Tech. Memor. No. 92, NRCC No. 9851*, Laval University, Quebec, National Research Council of Canada, Canada, 79–87.
- Freudenthal, A.M. (1956). "Physical and statistical aspects of fatigue." in *Advance in Applied Mechanics*, Vol. 4, Academic Press, 117–157.
- Freudenthal, A.M. (1968). "Statistical approach to brittle fracture." Chapter 6 in *Fracture*, Vol. 2, ed. by H. Liebowitz, Academic Press, 591–619.

- Freudenthal, A.M., and Gumbell, E.J. (1956). "Physical and statistical aspects of fatigue." in *Advances in Applied Mechanics*, Vol. 4, Academic Press, 117-157.
- Galileo, Galilei Linceo (1638). "Discorsi i Dimostrazioni Matematiche intorno à due Nuove Scienze, Elsevirii, Leiden; English transl. by T. Weston, London (1730), pp. 178-181.
- Gettu, R., Bažant, Z.P., and Karr, M.E. (1990). "Fracture properties and brittleness of high-strength concrete", *ACI Materials Journal* 87 (Nov.-Dec.), 608-618.
- Griffith, A.A. (1921). "The phenomena of rupture and flow in solids." *Phil. Trans.*, 221A, 179-180.
- Hillerborg, A., Modéer, M. and Petersson, P.E. (1976). "Analysis of crack formation and crack growth in concrete by means of fracture mechanics and finite elements." *Cement and Concrete Research* 6 773-782.
- Iguro, M., Shiyao, T., Nojiri, Y., and Akiyama, H. (1985). "Experimental studies on shear strength of large reinforced concrete beams under uniformly distributed load, *Concrete Library International, Japan Soc. of Civil Engrs.* No. 5, 137-154 (translation of 1984 article in Proc. JSCE).
- Kaplan, M.F. (1961). "Crack propagation and the fracture concrete", *ACI J.*, V. 58, No. 11.
- Kerr, A.D. (1996). "Bearing capacity of floating ice covers subjected to static, moving, and oscillatory loads." *Appl. Mech. Reviews*, ASME 49 (11), 463-476.
- Kesler, C.E., Naus, D.J., and Lott, J.L. (1971). "Fracture Mechanics—Its applicability to concrete", *Proc. Int. Conf. on the Mechanical Behavior of Materials*, Kyoto, The Soc. of Mater. Sci., Vol. IV, 1972, pp. 113-124.
- Kittl, P. and Diaz, G. (1988). "Weibull's fracture statistics, or probabilistic strength of materials: state of the art." *Res Mechanica*, 24, 99-207.
- Kittl, P. and Diaz, G. (1990). "Size effect on fracture strength in the probabilistic strength of materials." *Reliability Engrg. Sys. Saf.*, Vol. 28, 9-21.
- Lei, Y., O'Dowd, N.P., Busso, E.P., and Webster, G.A. (1998). "Weibull stress solutions for 2-D cracks in elastic and elastic-plastic materials." *Int. J. of Fracture* 89, 245-268.
- Leicester, R.H. (1969). "The size effect of notches", *Proc., 2nd Australasian Conf. on Mech. of Struct. Mater.*, Melbourne, pp. 4.1-4.20.
- Li, Zhengzhi, and Bažant, Z.P. (1998). "Acoustic emissions in fracturing sea ice plate simulated by particle system." *J. of Engrg. Mechanics ASCE* 124 (1), 69-79.
- Lichtenberger, G.J., Jones, J.W., Stegall, R.D., and Zadow, D.W. (1974). "Static ice loading tests Resolute Bay—Winter 1973/74." *APOA Project No. 64, Rep. No. 745B-74-14, (CREEL Bib. No. 34-3095)*, Sunoco Sci. and Technol., Richardson, Texas.
- Mariotte, E. (1686). *Traité du mouvement des eaux*, posthumously edited by M. de la Hire; Engl. transl. by J.T. Desvaguliers, London (1718), p. 249; also *Mariotte's collected works*, 2nd ed., The Hague (1740).
- Marti, P. (1989). "Size effect in double-punch tests on concrete cylinders," *ACI Materials Journal* 86, No. 6, 597-601.
- Mihashi, H. (1983). "Stochastic theory for fracture of concrete." *Fracture mechanics of concrete*, F.H. Wittmann, ed., Elsevier Science Publishers, B.V., Amsterdam, The Netherlands, 301-339.
- Mihashi, H. and Izumi, M. (1977). "Stochastic theory for concrete fracture." *Cem. Concr. Res.* 7, 411-422.
- Mihashi, H., Okamura, H., and Bažant, Z.P., Editors (1994). *Size effect in concrete structures* (Proc., Japan Concrete Institute Intern. Workshop held in Sendai, Japan, Oct.31-Nov.2, 1995). E & FN Spon, London-New York.
- Mihashi, H., and Rokugo, K., eds. (1998). *Fracture Mechanics of Concrete Structures* (Proc., 3rd Int. Conf., FraMCoS-3, held in Gifu, Japan), Aedificatio Publishers, Freiburg, Germany
- Mihashi, H. and Zaitsev, J.W. (1981). "Statistical nature of crack propagation," Section 4-2 in *Report to RILEM TC 50—FMC*, ed. F.H. Wittmann.
- Okamura, H. and Maekawa, K. (1994). "Experimental study of size effect in concrete structures, in *Size effect in concrete structures*", ed. by H. Mihashi, H. Okamura and Z.P. Bažant, E & FN Spon, London, 3-24. (Proc., JCI Intern. Workshop, held in Sendai, Japan, 1993).
- Peirce, F.T. (1926). *J. Textile Inst.*, 17, 355.
- Petersson, P.E. (1981). "Crack growth and development of fracture zones in plain concrete and similar materials." *Report TVBM-1006*, Div. of Building Materials, Lund Inst. of Tech., Lund, Sweden.

- Planas, J. and Elices, M. (1988). "Conceptual and experimental problems in the determination of the fracture energy of concrete," *Proc. Int. Workshop on "Fracture Toughness and Fracture Energy, Test Methods for Concrete and Rock*, Tohoku Univ., Sendai, Japan, pp.203-212.
- Planas, J. and Elices, M. (1989). in *Cracking and Damage*, ed. by J. Mazars and Z.P. Bažant, Elsevier, London, 462-476.
- Planas, J., Elices, M., and Guinea, G.V. (1993). "Cohesive cracks vs. nonlocal models: Closing the gap." *Int. J. of Fracture*, **63**(2), 173-187.
- RILEM (1990) Recommendation. "Size effect method for determining fracture energy and process zone of concrete." *Materials and Structures* **23**, 461-465.
- Rosen, B.W. (1965). "Mechanics of composite strengthening." *Fiber Composite Materials*, Am. Soc. for Metals Seminar, Chapter 3, American Society for Metals, Metals Park, Ohio, 37-75.
- Ruggieri, C., and Dodds, R.H. (1996). "Transferability model for brittle fracture including constraint and ductile tearing effects—a probabilistic approach." *Int. J. of Fracture* **79**, 309-340.
- Sedov, L.I. (1959). *Similarity and dimensional methods in mechanics*. Academic Press, New York.
- Selected Papers by Alfred M. Freudenthal* (1981). Am. Soc. of Civil Engrs., New York.
- Shioya, Y. and Akiyama, H. (1994). "Application to design of size effect in reinforced concrete structures." in *Size Effect in Concrete Structures* (Proc. of Intern. Workshop in Sendai, 1993), ed. by H. Mihashi, H. Okamura and Z.P. Bažant, E & FN Spon, London, 409-416.
- Tippett, L.H.C. (1925). "On the extreme individuals and the range of samples", *Biometrika* **17**, p. 364.
- von Mises, R. (1936). "La distribution de la plus grande de n valeurs." *Rev. Math. Union Interbalcanique* **1**, p. 1.
- Walraven, J., and Lehwalter (1994). "Size effects in short beams loaded in shear", *ACI Structural Journal* **91** (5), 585-593.
- Walraven, J. (1995). "Size effects: their nature and their recognition in building codes", *Studi e Ricerche* (Politecnico di Milano) **16**, 113-134.
- Walsh, P.F. (1972). "Fracture of plain concrete." *Indian Concrete Journal* **46**, No. 11.
- Walsh, P.F. (1976). "Crack initiation in plain concrete." *Magazine of Concrete Research* **28** 37-41.
- Weibull, W. (1939). "The phenomenon of rupture in solids." Proc., Royal Swedish Institute of Engineering Research (Ingenioersvetenskaps Akad. Handl.) **153**, Stockholm, 1-55.
- Weibull, W. (1949). "A statistical representation of fatigue failures in solids." *Proc., Roy. Inst. of Techn.* No. 27.
- Weibull, W. (1951). "A statistical distribution function of wide applicability." *J. of Applied Mechanics ASME*, Vol. 18.
- Weibull, W. (1956). "Basic aspects of fatigue." *Proc., Colloquium on Fatigue*, Stockholm, Springer-Verlag.
- Williams, E. (1957). "Some observations of Leonardo, Galileo, Mariotte and others relative to size effect." *Annals of Science* **13**, 23-29.
- Wisnom, M.R. (1992). "The relationship between tensile and flexural strength of unidirectional composite." *J. of Composite Materials*, **26**(8), 1173-1180.
- Wittmann, F.H., Editor (1995). *Fracture Mechanics of Concrete Structures* (Proc., 2nd Int. Conf. on Fracture Mech. of Concrete and Concrete Structures (FraMCoS-2), held at ETH, Zürich), Aedificatio Publishers, Freiburg, Germany, 515-534 (1944 pp.)
- Wittmann, F.H. and Zaitsev, Yu. V. (1981). "Crack propagation and fracture of composite materials such as concrete." *Proc., 5th Int. Conf. on Fracture (ICF5)*, Cannes.
- Zaitsev, J.W., and Wittmann, F.H. (1974). "A statistical approach to the study of the mechanical behavior of porous materials under multiaxial state of stress," *Proc. of the 1973 Symp. on Mechanical Behavior on Materials*, Kyoto, Japan, 705 p.
- Zech, B. and Wittmann, F.H. (1977). "A complex study on the reliability assessment of the containment of a PWR, Part II. Probabilistic approach to describe the behavior of materials." *Trans. 4th Int. Conf. on Structural Mechanics in Reactor Technology*, T.A. Jaeger and B.A. Boley, eds., European Communities, Brussels, Belgium, Vol. H, J1/11, 1-14.